CHALMERS
UNIVERSITY OF TECHNOLOGY

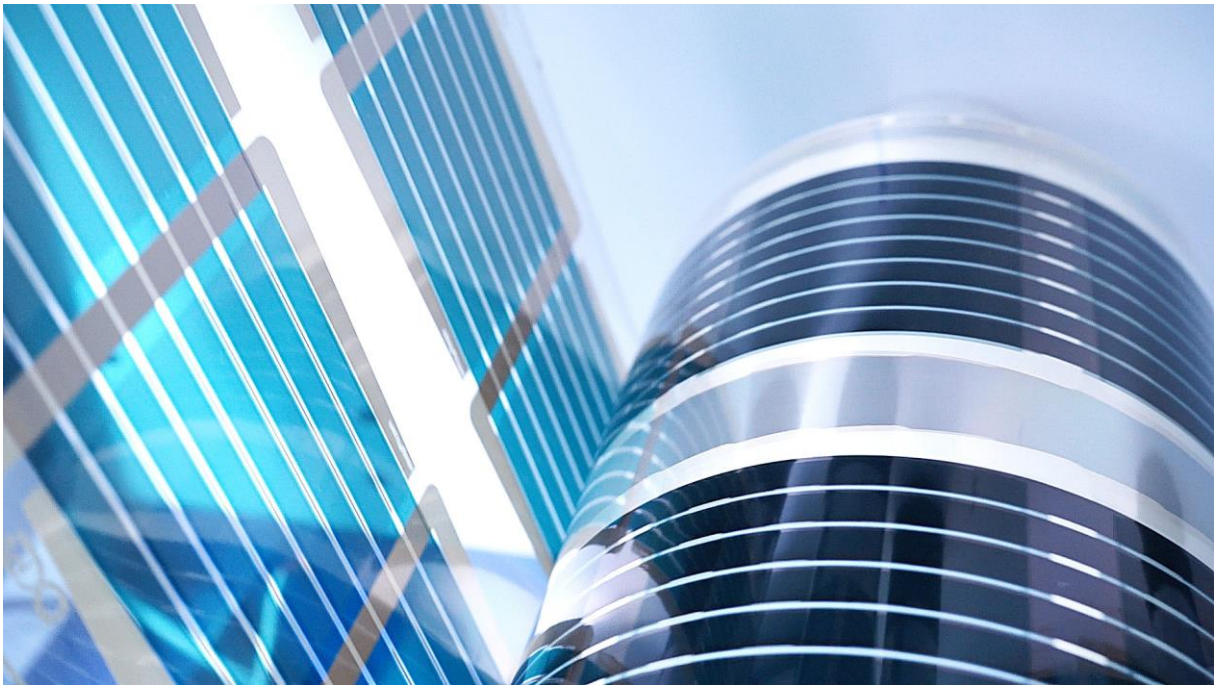

Life Cycle Assessment of a Low-Metal Organic Solar Cell

Master's thesis in Industrial Ecology

MINNEA HOLM

Department of Technology Management and Economics
Division of Environmental Systems Analysis
CHALMERS UNIVERSITY OF TECHNOLOGY
Gothenburg, Sweden 2020
Report No. E2020:002

MASTER'S THESIS E 2020:002

Life Cycle Assessment of a Low-Metal Organic Solar Cell

MINNEA HOLM

Tutor, Chalmers: Rickard Arvidsson

Department of Technology Management and Economics
Division of Environmental Systems Analysis
CHALMERS UNIVERSITY OF TECHNOLOGY

Gothenburg, Sweden 2020

Life Cycle Assessment of a Low-Metal Organic Solar Cell

MINNEA HOLM

Master's Thesis E2020:002

Department of Technology Management and Economics
Division of Environmental Systems Analysis

Chalmers University of Technology

SE-412 96 Gothenburg, Sweden

Telephone + 46 (0)31-772 1000

Cover photography:

InifnityPV, https://infinitypv.com/press/downloads. Please note that aside from granting me the right to use their picture for the cover, InfinityPV has no connection to this thesis, and the OPV depicted is not the one this LCA investigates.

Chalmers digitaltryck,

Gothenburg, Sweden 2020

Abstract

Recent developments in the field of photovoltaic technology have led to the creation of a new type of thin-film solar cell called organic photovoltaic (OPV). Unlike other thin-film solar cells, it is not dependent on scarce or toxic materials. In addition, OPVs can be produced rapidly and energy efficiently through continuous (roll-to-roll) processing. This gives OPVs an advantage compared to the already established photovoltaic technologies that either require a large amount of energy for their manufacturing or contain scarce and toxic materials. Previous studies have predicted that the energy payback time (EPBT) of OPV cells can be as little as a few days, compared to three to four years for the most common type of solar cell on the market.

However, as OPV is under development, the environmental impact and EPBT differs significantly depending on the OPV technology applied. In this study, the environmental impacts and the EPBT of a specific low-metal OPV technology, here called OPV-C, is explored using life cycle assessment. The production is currently on pilot-scale, but it is planned to be scaled up in the near future. The functional unit of the study was 1 m^2 active area OPV-C. The results show that the plastic substrate encapsulating the solar cell is responsible for 90% of the cumulative energy demand (CED) (in total 900 MJ_{eq} per m^2 active area), and it is the largest contributor to all the environmental impact categories considered. This is because the substrate is treated with a thin protective barrier in an energy-intensive sputtering process. The sputtering process uses electrical energy, which is why the electricity mix applied is critical for the final environmental impact. Two scenarios were created, one with a German electricity mix and one with a Swedish electricity mix. These were chosen to show the difference in the results when using electricity with different carbon footprints. The location of the barrier substrate production is unknown, although suppliers has several manufacturing sites in Germany. When a German electricity mix, which has a relatively high carbon footprint, is applied in the sputtering process, the contribution to climate change equals 53 kg CO_2 equivalents per m^2 active area. If instead a Swedish electricity mix is applied in the sputtering process, the emissions are less than 5 kg CO_2 equivalents for the same area. This shows not only the impact of the electricity mix, but also that the overall impact from the sputtering is very large, as nothing but this process was changed between the two scenarios.

For calculating the EPBT, a hypothetical scenario of future large-scale electricity production was applied. In this scenario, where 10 years lifetime of the solar cell and an average-world insolation was assumed, the EPBT is 16 months for an OPV-C cell with 5% efficiency, and eight months for an OPV-C cell with 10% efficiency. For the same scenario, the energy return factor (ERF) was 7.6 for a module with 5% efficiency and 15.1 for a module with 10% efficiency, meaning that the OPV-C cell can either return 7.6 or 15.1 times the invested energy throughout its lifetime, depending on the efficiency of the cell.

Keywords: Organic solar cells, Organic photovoltaics, OPV, Thin-film, Life cycle assessment.

Acknowledgements

I would like to express my deepest gratitude to everyone who has provided we with helpful information and support throughout the course of this thesis work. First, I would like to thank my examiner and supervisor, Rickard Arvidsson, and my supervisor, Anna Furberg, for their time and the invaluable advice they have provided. I would also like to thank everyone from the commissioner for providing me with useful information. Lastly, I would like to thank my family and friends for their support.

Contents

1 Introduction

1.1 Background

Photovoltaic (PV) systems, more commonly known as solar power systems, are becoming increasingly popular as the technology offers great opportunities for both small and large scale renewable energy production. There are several different types of solar power systems on the market, the most common being crystalline silicon cells (Schmidt-Mende & Weickert, 2016). Silicon-based solar cells are the most well-established technology on the market. It has had time to mature and reach increasing levels of efficiency in parallel with lower production costs. Another common type of solar cells is thin-film solar cells, such as the amorphous silicon (a-Si), copper indium gallium selenide (CIGS) and cadmium telluride (CdTe) solar cells (Lee & Ebong, 2017).

Although these types of conventional solar cells have reached a mature level on the market, they have drawbacks either because of their energy intense manufacturing (silicon solar cells) or because that they consist of toxic and/or scarce materials (most types of thin-film solar cells). The high energy intensity of silicon solar cell production is for example reflected by the fact that despite their high efficiency rate, silicon solar cells have an energy payback time (EPBT) in the range of 1-2 years (Espinosa et.al., 2011). The EPBT is the time it takes for a solar cell to produce as much energy as its production initially required. These drawbacks of conventional solar cells contribute to problems related to material scarcity as well as human health and environmental impacts (Grandell & Höök, 2015).

A new type of solar cells called organic photovoltaic (OPV) or organic solar cells have emerged as an alternative to the conventional ones. OPVs are based on organic semiconductors that absorb the incoming light (Geiker & Andersen, 2009). The active layers of an OPV are made from conductive organic polymers or organic molecules. OPVs generally do not reach the same level of efficiency as the more traditional types of solar PVs, but they have other advantages. Although some types of OPV cells contain scarce metals, such as silver or indium in the electrodes, the OPV technology is less dependent on scarce and toxic materials compared to other thin-film technologies (Grandell & Höök, 2015). In addition, OPV cells require significantly less energy in their manufacturing since they can be produced highly efficiently through a roll-to-roll process. Thus, OPV can have very short EPBTs, in the range of weeks or even days, as well as a low production cost (Espinosa et.al., 2011).

As the OPV technology has advanced, new application opportunities have emerged. One such opportunity is using organic solar cells instead of batteries in indoor devices, where the solar cell harvest light from lamps. This study focuses on the environmental impact of small-scale OPV, mainly intended for such indoor applications. The studied OPV is a recently developed technology where metal components in the electrode, such as indium and silver, have been replaced with carbon. They thus receive a lower metal content and a higher carbon content, why they will here be referred to as OPV-C, with C standing for carbon. The fact that these solar cells consist of non-toxic elements and are produced through fast and low-energy manufacturing processes, indicates that the product could have a low environmental impact and a short EPBT compared to silicon solar cells and other types of thin-film technologies on the market. However, whether this is the case has not yet been fully investigated for this specific, low-metal OPV technology.

1.2 Aim and Research Questions

The aim of this master's thesis project is to conduct a life cycle assessment (LCA) on the OPV-C technology. The goal is to investigate the environmental impact of the solar cells, in relation to a functional unit. The results of the LCA will be presented in a way that ensures comparability with LCA studies on other OPVs.

The current production is pilot-scale. As the OPV-C technology becomes more developed, larger solar cells might soon be produced. Therefore, aspects such as production efficiency and waste generation, which need to be taken into account in order to make the LCA applicable for future production, are considered. For this reason, the scalability of the solar cell production will also be reflected upon.

The specific research questions are:

1. What is the environmental impact of OPV-C cells?
2. What is their EPBT?

2 Life Cycle Assessment

An LCA includes a product's total life cycle, from raw material acquisition and manufacturing, to transport, use and waste management (Finnveden et al., 2009). The assessment includes ingoing resources as well as outgoing emissions to the environment, and can be used to pinpoint environmental hotspots in a products life cycle (Hellweg & Canals, 2014). A general life cycle model is illustrated in Figure 1.

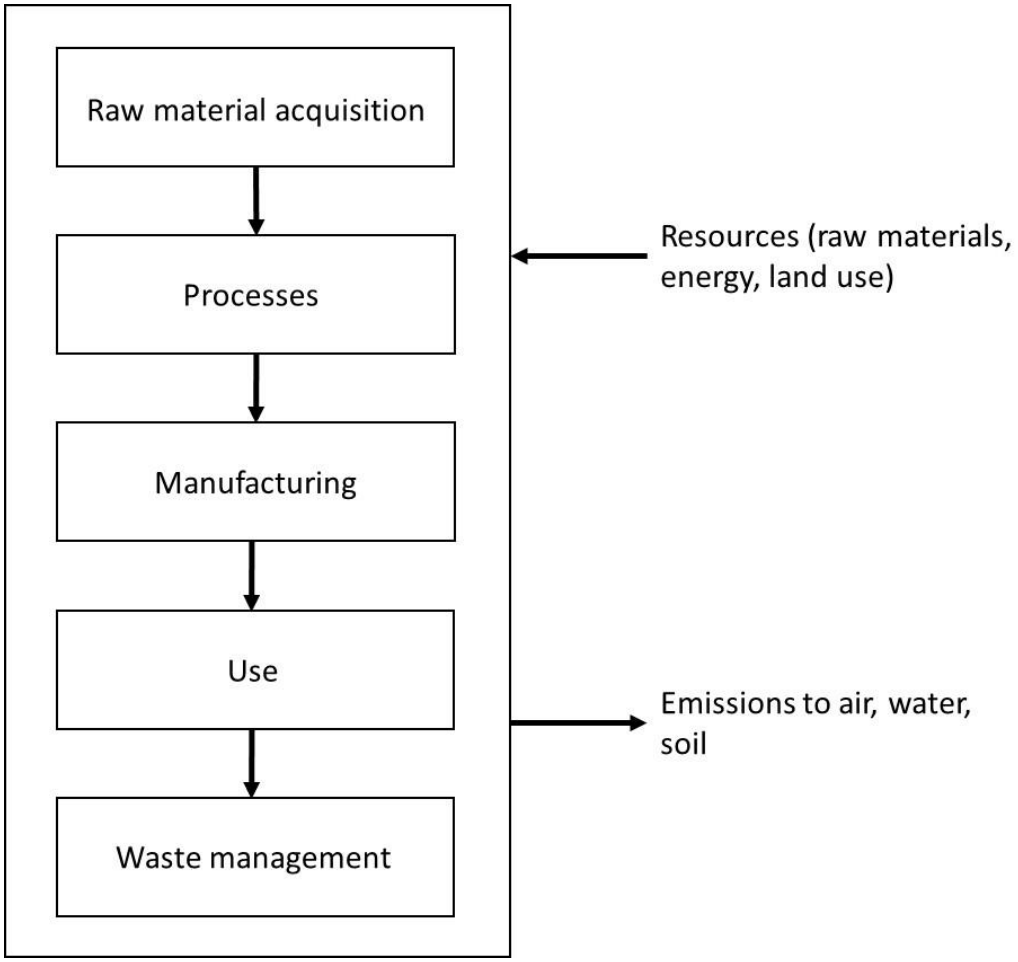

Figure 1. The life cycle model. In addition, transportations steps might be present. Arrows represent flows (product flows inside the box and elementary flows outside the box). Adapted from Baumann & Tillman (2004).

The reason for undertaking an LCA is usually the desire to understand the environmental impact of a product. The goal can either be to answer a question such as "what is the environmental impact associated with this product?" (an attributional LCA), or to answer a question such as "what will be the environmental consequences of a certain action?" (a change-oriented or consequential LCA) (Baumann & Tillman, 2004; Finnveden et al., 2009).

An LCA can also be considered a set of procedural steps describing how to study the environmental impact of a product. As mentioned by Baumann and Tillman (2004), the four main steps in an LCA are (1) the *goal and scope definition*, (2) the *inventory analysis*, (3) the *impact assessment* and (4) the *interpretation*. As can be seen in Figure 2, an LCA is an iterative process, meaning that steps and decisions should be repeated and modified as additional information is acquired.

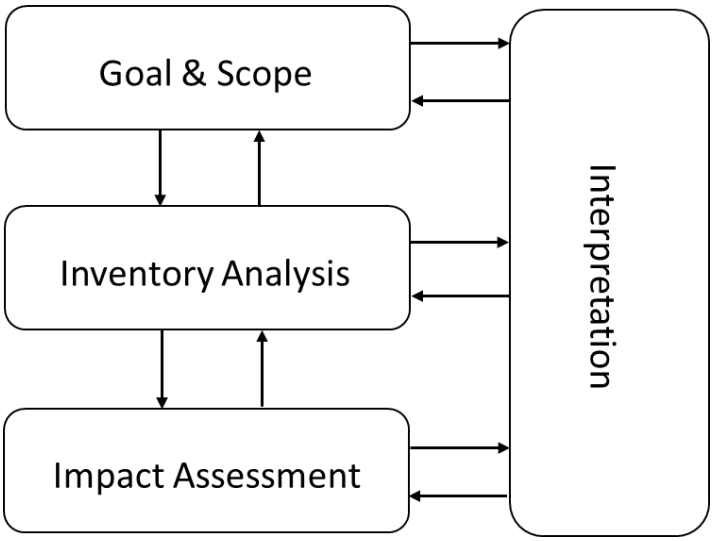

Figure 2. The LCA framework. Adapted from Baumann & Tillman (2004).

In the goal and scope definition, the studied product and the aim of the study are decided upon (Baumann & Tillman, 2004). There are two main actors involved in this step: the commissioner and the practitioner. The commissioner is the actor that initiates the study, whereas the practitioner is the actor that performs the study. It is the commissioner that states the goal of the study, whereas the practitioner is responsible for reaching that goal by using appropriate methodologies. The commissioner and practitioner should work together to decide upon a goal and scope definition that focuses on the right questions to reach the goal set by the commissioner. The goal of the study should be stated so that it clearly explains the intended application and audience of the study, as well as the reason for why the study is being carried out. In the scope definition, the functional unit, system boundaries and allocation method are chosen. For this step, it can be helpful to create an initial flowchart of the system.

The inventory analysis is the second step of conducting an LCA. Here, a flow model is created, representing an incomplete mass and energy balance of the system. The reason the mass balance is incomplete, is because only environmentally relevant flows are considered. The creation of a life cycle inventory (LCI) includes the construction of a flowchart in relation to the system boundaries, data collection and calculation of environmental loads in relation to the functional unit (Baumann & Tillman, 2004).

The third step of the LCA is the life cycle impact assessment (LCIA). This is where the environmental loads defined in the inventory analysis are "translated" into environmental impacts. As an example, the emission of sulphur dioxide (SO_2) is translated into impacts on acidification. This is done to get an understanding of what the effects of the emissions are and to make the results more comprehensible by going from often >100 emissions and recourses to ~10 impact categories. Thus, the impact categories are defined and then the results from the inventory analysis are classified, i.e. assigned to their respective impact categories. Then, the environmental impact is calculated for each category, i.e. characterized, followed by grouping, where the indicators are sorted and possibly ranked. Next, the results can optionally be further aggregated, which is called weighing. Lastly, the data quality is analysed, using a sensitivity analysis. This is to create a better understanding of the reliability of the results.

In parallel with the previously mentioned steps, the results are interpreted, and the robustness is tested. This means that conclusions are drawn, and the results are refined and presented in an understandable way. The most important results can be presented in different types of diagrams, such as bar diagrams. How the results are presented depends on the intended audience and the goal of the study. For example, if the audience is knowledgeable within the field of LCA and the technology being investigated, the results can be less aggregated than if the audience is unfamiliar with the field.

3 Technical Description of OPV Cells

In this section, the technology of general OPV cells is described, including their working principle, solar cell structures, materials applied in solar cells, their fabrication and the current state of development.

3.1 Working Principle

Organic solar cells, as well as other solar cells, work through the photovoltaic effect. In the photovoltaic effect, sunlight, which is electromagnetic radiation consisting of photons, is converted into electrical energy. Electricity generation from organic solar cells occurs through the following steps: light absorption, exciton diffusion, charge separation and charge extraction (Marinova, Valero, & Delgado, 2017). When photons hit the surface of the solar cell, they travel through the transparent electrode and become absorbed by the active layer. The photons reaching the active layer have a higher energy than the semiconductor band gap. This makes an electron excite to an unoccupied state above the band gap, which generates an exciton bound electron-hole pair. Next, the electron-hole pair diffuses (separates) through a phase boundary between the donor and acceptor. The phase boundary is a built-in gradient in the electrochemical potential of the solar cell. Due to the resistance in the active layer, the electron travels towards the negative electrode, while the hole travels to the positive electrode. As the positive and negative charge strive to recombine, but the resistance within the solar cell is too high, they recombine by letting the electron travel through an external circuit, known as charge extraction. Thus, electricity is generated (Marinova et al., 2017).

3.2 Solar Cell Structures

One of the main differences between different solar cell types lie in the structure of the cells. Three general structures of solar cells are presented in Figure 3. As can be seen, all cells have one negative electrode (cathode) and one positive electrode (anode). Between the electrodes, there are a hole transport layer (HTL), an active layer and an electron transport layer (ETL). The active layer consists of two materials, a polymer donor, which absorbs the light and has affinity for holes (a “space” for a missing electron), and an acceptor, which has affinity for electrons. The active material is a semiconductor, meaning that it acts both as a conductor and an insulator. The outer electrode needs to be transparent in order to let sunlight through.

There are three separate ways that the organic solar cells can be designed: the regular structure, with a transparent positive electrode, the inverted structure, where instead the negative electrode is transparent, and the tandem structure, which employs two (or more) active layers with complementary absorption (Marinova et al., 2017), see Figure 3. The idea of a tandem structure is that each active layer is tuned to absorb photons with different energies, typically a front cell with large band gap active layer to absorb incoming photons with high energies, and a back cell with low band gap active layer that absorbs low energy photons.

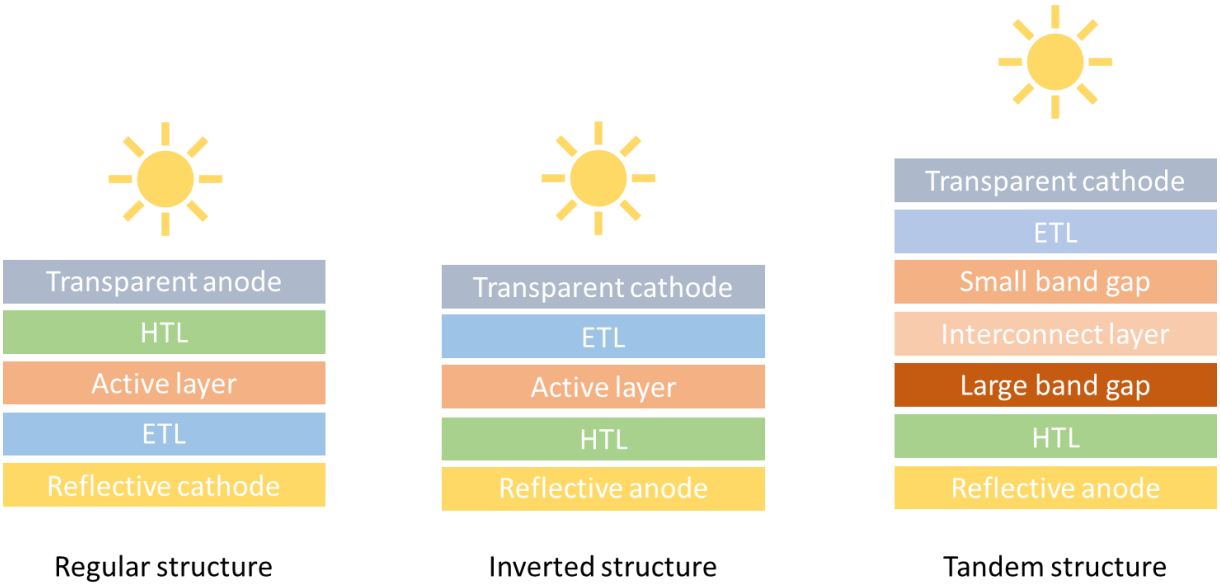

Figure 3. General OPV cell structures. HTL stands for hole transfer layer and ETL stands for electron transfer layer. Adapted from Marinova et al. (2017).

In addition to these structures, the donor and acceptor in the active layer can either be separated or blended. The separated version is called planar heterojunction (PHJ) and the blended is called bulk heterojunction (BHJ). In BHJ cells, the donor and acceptor have a larger interface area, which increases exciton diffusion. This in turn increases the efficiency of the solar cell (Marinova et al., 2017).

3.3 Materials

Another main difference between different solar cell types is related to the materials that are applied. Organic solar cells are primarily made from polymer materials. As will be described in more detail in Section 5.1 all layers of an OPV cell are deposited in the form of inks, containing e.g. polymer materials, where the active materials are dispersed in various kinds of solvents. As the solvents can differ widely depending on the producer and mostly evaporate during the drying processes, this section focuses on the photoactive materials that remain present in the OPV cells during their use.

3.3.1 Electrodes

One commonly used material for the front electrode is indium-tin oxide (ITO) (Krebs, dos Reis Benatto, Laurent, Hösel, & Espinosa, 2015). It is technically very well suited for OPV as it can be deposited in the form of a thin and transparent layer and it has good electronic properties. However, using ITO for front electrodes has been identified as a bottleneck for large scale OPV production due to the scarcity of indium and the energy intensive manufacturing processes (Espinosa, García-Valverde, Urbina, & Krebs, 2011). A material that has proved to be promising for replacing ITO is silver, applied as grids, which can be used for both the front and the back electrode (Espinosa et al., 2012a). One benefit with using silver is that it can be easily recycled when the OPV cell has reached its end of life (EoL). Despite this advantage, silver is still a metal of similar scarcity as indium and when present in OPVs, it is also one of the main contributors to environmental impacts (Espinosa et al., 2013). Other potential materials for the front electrode are carbon, copper and aluminium. An LCA comparing these three materials as well as silver showed that the carbon-based OPV electrode had the lowest environmental impact (Krebs et al., 2015). However, although the modules with carbon-based front electrodes have

the same active area efficiency as ITO-based OPV, they require more sealing on the sides and have thus a less optimal area usage. This results in decreased overall module efficiency compared to ITO- and silver-based modules (Krebs et al., 2015). Different types of carbon has been investigated, including graphene, graphite and carbon nanotubes (García-Valverde, Cherni, & Urbina, 2010; Krebs et al., 2015; Song, Chang, Gradecak, & Kong, 2016).

For the back electrode, the same materials as for the front electrode can be used, but it does not necessarily need to be printed in a mesh pattern, as it does not need to let sunlight pass through. However, some manufacturers prefer their whole OPV cell to be transparent, in which case both electrodes need to be printed in a mesh pattern.

3.3.2 Electron and Hole Transport Layers

As mentioned in Section 3.1, the role of the ETL is to transport the excited electrons from the active layer to the negative electrode. Possible electrode transport layer materials in OPV cells are zinc oxide (ZnO), lithium fluoride (LiF), calcium (Ca), potassium hydroxide (KOH) and ethanolamine (MEA) (Espinosa, Hösel, Angmo, & Krebs, 2012b; Rafique, Abdullah, Sulaiman, & Iwamoto, 2018). For the HTL, PEDOT:PSS is the most widely used material. However, it does not show great stability in combination with ITO, thus metal oxides such as nickel oxide (NiO), vanadium oxide (V_2O_3), tungsten trioxide (WO_3) and molybdenum trioxide (MoO_3) have been employed (Rafique et al., 2018). Another material that has been found to function as HTL in BHJ cells is an oxidised form of graphene (GO) (Rafique et al., 2018). PEDOT:PSS and GO can also be used in a combination with metal oxides to circumvent material drawbacks.

3.3.3 Active Layer

Poly(3-hexylthiophene-2,5-diyl) (P3HT) and Phenyl-C61-butyric acid methyl ester (PCBM) are the two active layer materials that have been found in the literature (Espinosa et al., 2012a; Gevorgyan et al., 2017). PCBM is a fullerene derivative and a common electron donor material in OPVs, whereas P3HT acts as the acceptor. P3HT is a polymer. More information about P3HT and PCBM can be found in Section 5.2.5.

3.3.4 Additional Materials

Aside from the transport layers, active materials and electrodes, the solar cell requires a substrate onto which it can be printed. This can either be a plastic film or a glass substrate, depending on the needs of the manufacturer (Rafique et al., 2018). The substrate must be transparent and protect the solar cell from the environment. For roll-to-roll (R2R) processing, the substrate must be flexible why plastic film substrates are used (Krebs, 2009). Glass substrates require other types of manufacturing processes. Furthermore, an adhesive to seal the substrate around the layers of the solar cell and increase the protection from the environment is required (Espinosa et al., 2012a).

3.4 Roll-to-Roll Fabrication

As mentioned in Section 1, organic solar cells can be manufactured at high speed and low energy input. The use of R2R fabrication combined with solutions processing is one of the main advantages of organic solar cells. Roll-to-roll processing means that solar modules can be manufactured in a continuous process, where layers are being coated or printed onto a thin plastic film, which is rolled through one or several coating or printing steps, see Figure 4. The time to manufacture a rigid OPV cell (on a firm surface like glass) is measured in days, whereas the time to manufacture the same surface area of OPV through roll-to-roll processing is measured in seconds (Søndergaard, Hösel, Angmo, Larsen-Olsen, & Krebs, 2012).

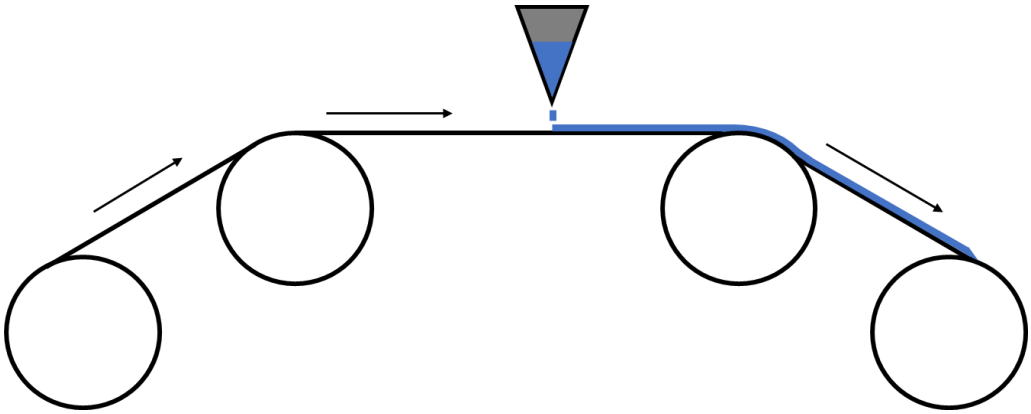

Figure 4. A schematic overview of a roll-to-roll process with ink deposition.

3.4.1 Coating and Printing Techniques

Coating and printing are the two main manufacturing steps in producing OPVs. Coating is a technique that allows to spread the ink that will become layers of the module in zero or one dimension on the thin film surface. In this setting, zero dimensions means that the ink is spread over the entire substrate, whereas one dimension would mean that stripes can be created with the ink on the substrate.

Some common coating techniques are blade coating (also known as knife coating or doctor blading), spray coating and slot-die coating (Søndergaard et al., 2012). In the blade coating process, an ink-filled reservoir supplies ink to the substrate surface where it is gradually deposited behind the knife. It is a zero-dimensional technique, meaning that it cannot be used to create patterns. This process has low losses of ink compared to comparable techniques (Krebs, 2009). Slot-die coating is a one-dimensional technique, as it is possible to create stripes on the coated surface. This is very suitable for creating multilayer solar cells with layered stripes of different materials. The ink is supplied through a pump and a slot, which allows to adjust the wet thickness through controlling the web speed, the ink supply or both (Krebs, Tromholt, & Jørgensen, 2010; Søndergaard et al., 2012). Spray coating is a coating method where ink forced onto the substrate through a nozzle, creating a fine aerosol. This method is zero-dimensional. In theory, a shadow mask could be used to create a pattern, but this is not likely to be useful outside of lab-scale (Søndergaard et al., 2012).

Printing techniques allows for ink formations of two, or even three, dimensions to be applied to the substrate. Printing means that an ink motif is being transferred from a solid form to a substrate. Most printing techniques use physical contact between the substrate and the object carrying the motif. Examples of common printing techniques using physical contact between the substrate and the object include screen printing, gravure printing and flexographic printing. One exception to this is inkjet printing, where droplets are released onto the substrate (Søndergaard et al., 2012). Some advantages of inkjet printing are that it has high resolution and uses a digital master, which means that the patterns can be changed with short setup times. This can be highly advantageous compared to other printing techniques where new cylinders must be produced whenever the printing pattern is changed.

3.5 Current State of Organic Photovoltaic Technologies

In addition to a fast and low-energy production process, OPV technologies may also have an advantage because they avoid the use of scarce metals such as lithium, copper and gold, as well as rare earth elements (REEs) that are commonly used in inorganic thin film solar cells (Than, 2018). However, there are several challenges to increase the market share of organic solar cells, such as increasing their power conversion efficiency and stability, i.e. the longevity of the solar modules. In a market setting, both the power conversion efficiency and stability of the OPVs need to be satisfactory and obtained at a low cost in order for the OPVs to become a well-functioning product for the customer (Krebs, 2009).

3.5.1 Energy Payback Time

The EPBT is an important parameter to optimize in making the OPVs competitive to conventional solar cells. In 2011, the EPBT for OPV cells were estimated to around 1.3-2.0 years (Espinosa, García-Valverde, & Krebs, 2011). In 2016, this number was decreased to 1.6-2.5 months for the solar conditions in southern Europe (Hengevoss, Baumgartner, Nisato, & Hugi, 2016). However, it has been estimated that the EPBT can become as low as one day (Espinosa et al., 2012b). To improve the EPBT, materials with a low embedded energy need to be selected, both active materials and solvents, in combination with increasingly efficient manufacturing processes.

3.5.2 Power Conversion Efficiency

In 2009, the record power conversion efficiency (PCE) for OPV cells were 7.6% (Buckley, 2009). The 2018 PCE record for fullerene-based OPV is 12.5%. For non-fullerene-based OPV using ITO as front electrode, a group of scientists made a record of 15% in April 2018 but managed to increase this to over 17% by the end of the year (Meng et al., 2018; Newman, 2018). Commercial silicon solar cells generally perform in the range of 18-22% (Bourzac, 2018).

3.5.3 Stability

Another important aspect is the stability of the solar cell. OPVs are prone to decomposition and thus do not perform as well as other types of solar cells when it comes to longevity, an aspect which is seen as a bottleneck for their commercialization (Rafique et al., 2018). There is also a challenge in translating laboratory-scale results into a mass-production setting. The ratio between the ingoing energy during production and the solar cell's lifetime energy production is sometimes used as a performance indicator, called the energy return factor (ERF) (Espinosa, García-Valverde, Urbina, et al., 2011). Improving the PCE and the stability is necessary to maximise the net energy production over a solar cell's lifetime.

4 Goal and Scope Definition

The goal of this study is to assess the environmental impact of the OPV-C technology and to investigate the EPBT of the OPV-C cells. In addition, the results of the impact assessment will, when possible, be compared with other OPVs available on the market. The study is conducted on the behalf of a commissioner whose name is omitted for reasons of confidentiality. This LCA is attributional, as it focuses on assessing the environmental impact associated with a product. The results can be used to support marketing and product development of OPV-C cells. In addition, the audience includes, aside from the commissioner, anyone interested in the development of OPVs.

4.1 Functional Unit

The functional unit in this study is 1 m^2 of active solar cell area. This is chosen in order to make it easy to apply the results to solar cells of different sizes and in different applications. In addition, this functional unit increases the comparability with similar studies, as other LCAs on OPV express their results in terms of area as well. The reference flow in the inventory analysis, however, is 1 m^2 *processed* area, with 70% *active* area. This reference flow was chosen because some proxy data has been assembled for the manufacturing processes, and this proxy data was typically given per 1 m^2 processed area.

It has been recommended that the functional unit for solar PVs is set to 1 kWh of generated electricity (Raugei, Fthenakis, & Kim, 2011). However, this requires assumptions regarding the total electricity generation for the solar cell. Although the PCE and expected indoor lifetime is known for OPV-C, the insolation during the cell's lifetime is not known in this study. Assumptions regarding insolation and irradiation are here only applied for a theoretical large-scale case to present potential results related to electricity production.

4.2 System Boundaries

The product system is divided into a foreground system and a background system. The foreground system includes the processes that may be directly altered due to the results of this study. The background system includes all other modelled processes that would only indirectly be affected by measures taken. The foreground system includes the manufacturing process of OPV-C cells: ink preparation, ink deposition, drying, cutting and testing. The background system includes all related technical processes such as energy production, transportation and materials production, as well as the use phase and waste treatment. Figure 5 shows an overview over the processes included in this study, where the foreground system is marked in grey. Certain cut-off criteria are used, which means that some things related to the product life cycle is excluded from the assessment. In this study, production capitals such as machines and manufacturing sites, personnel and to some extent also the transportation steps included in the life cycle of an OPV-C cell are excluded. This is partly due to practicalities, as it is difficult to fully assess these subjects, and because the scope of the study does not cover changes in production capital. Another reason for excluding these aspects is the comparability to the results of similar LCAs, where similar cut-off criteria have been employed (Espinosa, García-Valverde, & Krebs, 2011; Espinosa et al., 2012a).

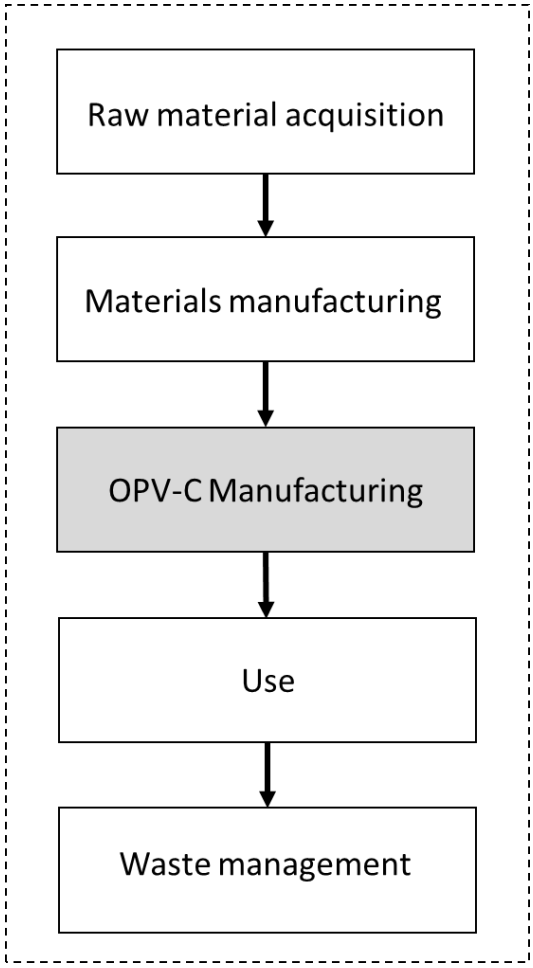

Figure 5. Overview of the product system. The foreground system is indicated in grey whereas the system boundary is shown with a dashed line.

4.3 Impact Categories and Impact Assessment

In order to evaluate the environmental impact of the OPV-C, a number of impact categories have been applied. The included impact categories are: cumulative energy demand (CED), climate change during the scope of 100 years (CC100), terrestrial ecotoxicity, (TETinf), freshwater eutrophication (FE), water depletion (WD) and freshwater ecotoxicity (FETinf). The impact assessment method of ReCiPe midpoint (hierarchic perspective) version 2008 was applied (Goedkoop et al., 2013).

4.3.1 Cumulative Energy Demand

Cumulative energy demand (CED) measures the total primary energy used to produce a product, in this case 1 m^2 active area OPV-C. This includes the direct process energy (recalculated to represent the corresponding amount of primary energy) in the foreground system, as well as the energy for materials manufacturing and raw materials extraction in the background system. This measure is especially useful for solar PV, as it is used in the calculation of the EPBT and ERF.

4.3.2 Climate Change 100 years

Climate change 100, also known as global warming, measures the climate change impact over 100 years that a product has during its life cycle. This is done by assessing the emissions of greenhouse gases and recalculating these emissions into carbon dioxide equivalents (CO_2 eq).

The climate change method of calculating climate impact was developed by the intergovernmental panel on climate change (IPCC) (Goedkoop et al., 2013)(Klöpffer, Mary, Curran, Hauschild, & Huijbregts Editors, 2015).

4.3.3 Terrestrial and Freshwater Ecotoxicity

Ecotoxicity is an impact category where the toxic effect of chemicals released during the life cycle is quantified (Goedkoop et al., 2013). It can be divided into different impact areas, such as water and land. The area of water can in turn be divided into the areas of freshwater and marine water. In this study, freshwater and terrestrial ecotoxicity is assessed.

4.3.4 Freshwater Eutrophication

Eutrophication is commonly associated with the release of nutrients to the environment, which leads to increased amounts of micro-organisms in the water environment. The breakdown of dead micro-organisms in turn lead to an increased oxygen consumption, which causes a lowering of the water oxygen levels that affects the ecosystems negatively.

4.3.5 Water Depletion

This impact category measures the total amount of water consumed in the life cycle as volume (e.g. cubic metres or litres) (Acero, Rodríguez, & Changelog, 2015).

4.4 Sources of Information and Software

Information about the studied OPV-C product, its ingoing materials and use, as well as relevant information regarding the background system, has been gathered directly from the commissioner. A literature study has also been conducted in scientific online databases and websites. Textbooks have been used for procedural information on how to conduct an LCA. Background system data have primarily been searched for in the online database Ecoinvent version 3.5 (Wernet, Bauer, Steubing, Reinhard, & Moreno-Ruiz, E. Weidema, 2016). The "cut-off by classification" allocation method has been applied. When background system data was unavailable in Ecoinvent, proxy information has been gathered mainly from other LCAs on organic solar cells.

5 Life Cycle Inventory Analysis

In this section, the inventories for the OPV-C cell are presented. Section 5.1 explains the manufacturing steps of the OPV-C cell, which can be seen in the grey box in Figure 6. In Section 5.2, the background system, which includes the production of ingoing materials, the use phase and waste treatment, are described in more detail.

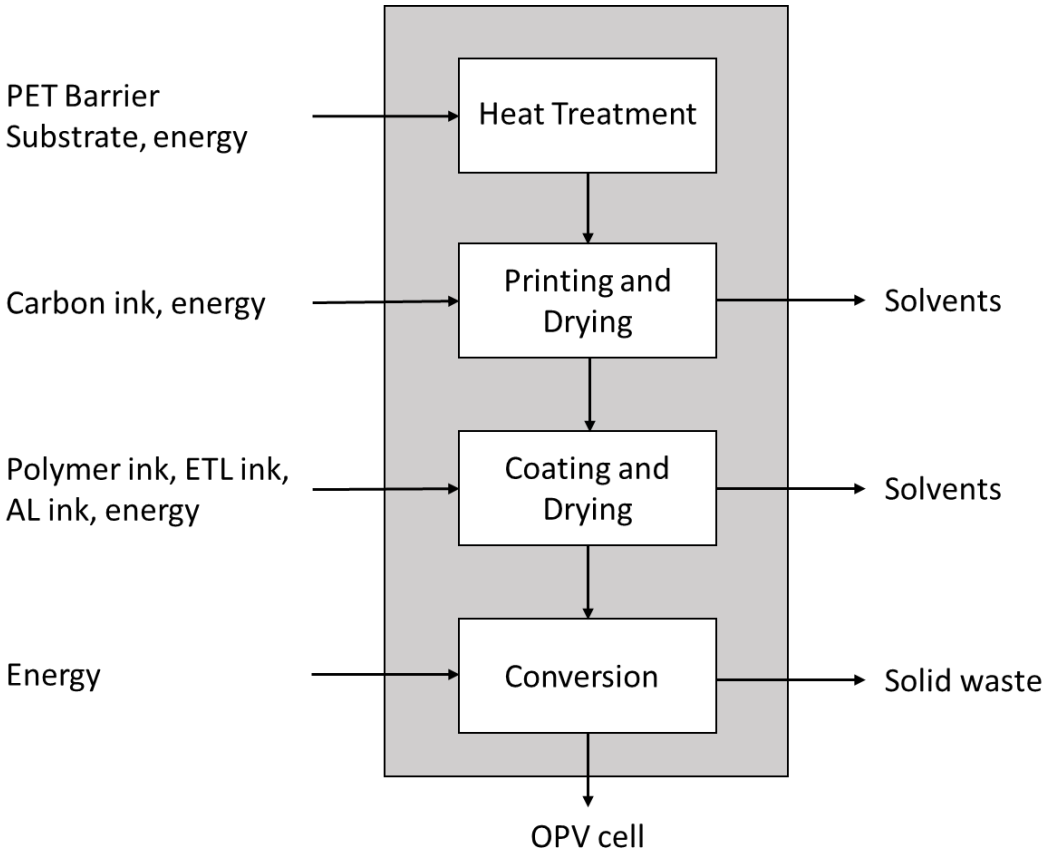

Figure 6. Detailed flowchart of the foreground system. PET: polyethylene terephthalate, ETL: electron hole transport layer, AL: active layer, OPV: organic photovoltaic.

5.1 OPV-C Manufacturing

The three main processes in OPV-C manufacturing are slot-die coating, rotary screen printing and drying. Only R2R processes are applied, meaning that the OPV-C is manufactured continuously. Despite efforts in finding product-specific energy input data for the processes, it could not be acquired. Thus, a literature study has been conducted, and energy inputs from studies on similar OPVs are used as proxy. All ingoing energy for the R2R processes is assumed to be electrical energy, as in other studies of OPVs (Espinosa et al., 2012b; Espinosa et al., 2013).

In all coating and printing processes, a 10% loss of the ingoing ink is assumed. The non-deposited ink (the 10% lost) is assumed to go to hazardous waste treatment. The layers are applied onto a polyethylene terephthalate (PET) barrier substrate, one at the time, with a drying step in between. The final layers (PEDOT:PSS, AL 1, AL 2, ETL and electrodes) of the solar cell are very thin, not adding any significant weight to the substrate. The layers can be seen in

Figure 7. In reality, the layers imbricate, meaning that they do not cover the whole active area, but rather overlap. In the final step of the manufacturing process, the conversion step, the substrate is folded lengthwise, making the striped layers fit together to create the final solar cell. This also explains the presence of two PEDOT-layers although only one deposition process has taken place – once the cell has been folded, there will be one PEDOT:PSS at the bottom and one at the top. The active area is 70%, which means that all layers except the carbon electrode cover 70% of the width of the substrate.

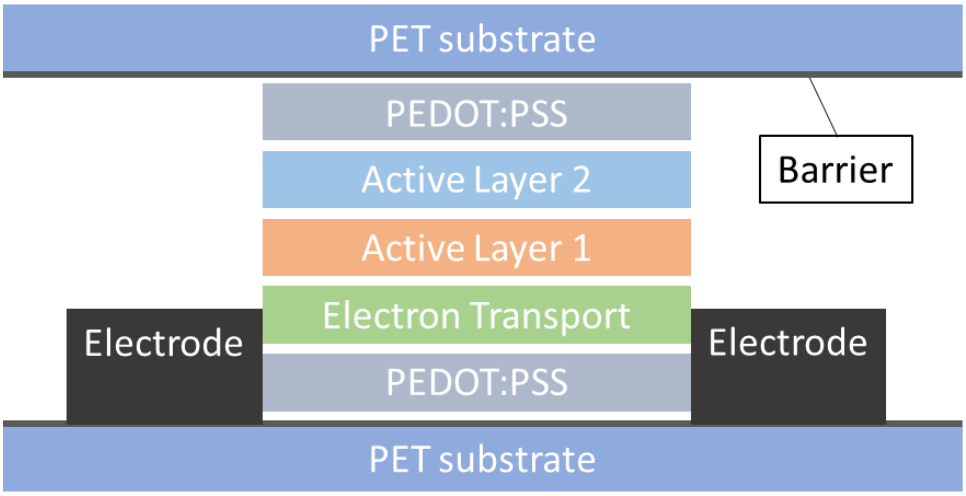

Figure 7. A schematic illustration of the cross-section of the solar cell assessed in this study. The figure is not to scale.

5.1.1 Heat Treatment and Drying Processes

The initial input into the manufacturing processes is a PET barrier substrate, consisting of a thin PET film with a metal oxide barrier for protection. The PET substrate production is explained in Section 5.2. The first process in the foreground system is heat treatment of the PET barrier substrate. For the heat treatment, a Kroenert printing and drying machine is used. The oven is 12 metres long and the substrate moves with 3 m/min, see Table 1. After the PET substrate has been prepared, layer deposition can be initiated. Due to the fact that energy use data from the actual printing and drying machine used is not available, proxy data are used. As the heat treatment and the first drying step are exact similar processes (in terms of oven length, temperature and speed), the same energy use proxy data are used for heat treatment as for the drying of carbon electrodes, see further Section 5.1.2.

Table 1. Drying processes.

Process	Oven length	Temperature	Speed
Heat treatment	12 m	120°C	3 m/min
Drying electrodes	12 m	120°C	3 m/min
Drying PEDOT	2 m	120°C	1 m/min
Drying ETL	2 m	100°C	1 m/min
Drying AL1 & 2	2 m	90°C	1 m/min

5.1.2 Rotary Screen Printing

The first layer to be added is the carbon electrode layer. The carbon ink is applied through rotary screen printing. The equipment used is a Kroenert printing and drying machine and a

rotary screen printer from Stork. As mentioned initially in Section 5.1, 10% of the ingoing ink is assumed to go to hazardous waste treatment. After the ink has been printed to the substrate, it is dried in the same machine in 120℃. During the drying process, the solvents are evaporated and emitted to air.

As mentioned in section 3.3.1, there are several different material choices for the electrodes. Due to fact that many OPV technologies use ITO or silver as electrode materials, only two LCAs where found that consider carbon electrodes and present the energy inputs for the rotary screen printing process, see Table 2. In Espinosa et al (2013), the study was performed at a pilot OPV factory at the Department of Energy Conversion and Storage at the Technical University of Denmark. They do not display any further information about the equipment used, however, the energy data for the manufacturing processes are taken directly from the site. Thus, the confidence in their data are considered high, but it is hard to assess whether it can be a good proxy for the manufacturing in this study. In the second article, by Espinosa et al. (2012b), there is more transparency regarding the equipment and the manufacturing conditions. They use a printing and coating machine from Grafisk Maskinfabrikk A/S. In addition, the machine includes an in-line rotary screen printing device from Stork.

Table 2. Energy requirements for electrode deposition through rotary screen printing. The chosen proxy data are taken from Espinosa et al. (2012b) (within thick lines).

Rotary Screen Printing of Carbon Electrodes, 1m^2 processed area				
Energy coating (Wh)	Energy drying (Wh)	Temperature drying	Mass per 1 m^2 (g)	Source
38	440	140℃	5.14	Espinosa et al. (2013)
11	250	140℃	4.59	Espinosa et al. (2012b)
-	-	120℃	4.2	This study

Consequently, none of the machinery can be proven to be exactly the same as the one used for the processes examined in this study. In addition, the results from the two studies vary quite significantly, by a factor of three for printing and almost a factor of two for drying, despite using the same processed area and drying temperature (Table 2). In Espinosa et.al. (2013), the working power of the oven is 12000 W, and the speed is between 0.2-2.5 m/min. Due to the fact that the analysis by Espinosa et al (2012b) is more transparent regarding equipment and condition, it is used as a proxy. The drying process differs by 20℃ and the speed is slower than in the actual drying processes in this study. This indicates that the estimation for energy use in the drying process is likely to be somewhat overestimated. However, the length of the oven and the residence time is not known. Aside from the machine used, other aspects that may have an impact on the total energy use for one meter processed area is the width of the substrate and the amount of ink being deposited. These factors were also considered when choosing the proxy data. The drying process is explained in Section 5.1.1.

5.1.3 Slot-die Coating

The second layer is the PEDOT-layer, which is added through slot-die coating. The PEDOT-layer is made from (1) PEDOT:PSS, which is a polymer commonly used in OPVs, (2) a surfactant, as well as (3) additional water and an alcohol as solvents. .PEDOT:PSS comes as a water-based solution from the supplier. The ingoing chemicals of the layer are produced by suppliers and mixed without heat to create the PEDOT:PSS ink. In total, approximately 20 g of PEDOT:PSS ink is deposited on 1 m^2 of processed area. In the subsequent drying process, the solvents are fully evaporated and emitted to air, as in all the drying processes.

Three LCA studies have been found to display the energy input for a PEDOT:PSS slot-die coating process (Espinosa et al., 2011; Espinosa et al., 2012a; Espinosa et al., 2012b). The PEDOT-layer is generally thicker than most other layers, meaning that it also requires more energy for the deposition process. As can be seen in Table 3, when significantly more ink is used, then the energy use in the process is also significantly higher. The slot-die PEDOT:PSS ink deposition process most similar to the OPV-C manufacturing of this study in terms of mass processed is the one in Espinosa et al. (2012b).

Table 3. Energy requirements for the slot-die coating of PEDOT-layer. The chosen proxy data for this study are taken from Espinosa et al. (2012b) (within thick lines).

Slot-die coating PEDOT-layer				
Energy Coating (Wh)	Energy drying (Wh)	Drying temp.	Mass per 1 m^2 (g)	Source
479	2300	-	73.64	(Espinosa et al., 2012a)
75	670	140°C	26.23	(Espinosa et al., 2012b)
455	2190	-	88.52	(Espinosa, García-Valverde, Urbina, et al., 2011)
-	-	-	19.99	This study

The ETL is added through slot-die coating as well. Its active material is a zinc oxide (ZnO), which is mixed with a solvent before the slot-die coating process. The solvents are evaporated to air during the drying process. In this step, 3.4 g of ZnO ink is deposited for every 1 m^2 of processed area. For this deposition process, the study most similar to the OPV-C manufacturing uses 109 Wh per m^2 of processed area (Espinosa, García-Valverde, Urbina, et al., 2011) (Table 4). This is based on the amount of ink going into the process and the active area of 67% in their study, which is close to the 70% used in this study. The drying process uses 328 Wh and 140°C, which is unfortunately a rather large leap from the 100°C in this study. Nevertheless, the amount of ingoing material and deposition area are similar.

Table 4. Energy requirements for the slot-die coating of electron transport layer. The chosen proxy data are taken from Espinosa et. al. (2011) (within thick lines).

Slot-die coating electron transport layer					
Energy Coating (Wh)	Energy drying	Drying temp.	Speed (m/min)	Mass per 1 m^2 (g)	Source
63	230	-	-	8.33	(Espinosa et al., 2013)
82	370	140°C	2.5	9.19	(Espinosa et al., 2012b)
109	330	140°C	2.0	5.23	(Espinosa, García-Valverde, Urbina, et al., 2011)
-	-	100°C	2.5	3.42	This study

The AL 1 & 2 ink is added through slot-die coating. Again, the solvent is emitted to air during the drying process.

Four LCA studies have similar processes for the AL preparation and deposition as this study (Espinosa, García-Valverde, Urbina, et al., 2011; Espinosa et al., 2012a; Espinosa et al., 2012b; Espinosa et al., 2013) (Table 5). These studies all have about 7 g of ink per m^2 processed area. Taking the active area into account, two of the studies are very similar to this one, and they are both very similar in energy use for the total process, including drying (Espinosa et al., 2011; Espinosa et al., 2012a). The article with the processes most similar to the ones in this study uses 6.9 Wh for the preparation process, 72 Wh for the deposition process and 345 Wh for the drying process.

Table 5. Energy requirements for the slot-die coating of one active layer. The chosen proxy data for this study are taken from Espinosa et al. (2012a) (within thick lines).

Slot-die coating active layer						
Ink Preparation (Wh)	Energy Coating (Wh)	Energy drying (Wh)	Drying temp.	Mass per 1 m^2 (g)	Active area	Source
6.8	27	230	-	7.46	45.53%	(Espinosa et al., 2013)
6.9	72	350	-	7.08	68.10%	(Espinosa et al., 2012a)
5.6	41	370	140°C	6.34	45%	(Espinosa et al., 2012b)
6.6	68	320	140°C	7.30	67%	(Espinosa, García-Valverde, Urbina, et al., 2011)
-	-	-	90°C	7.30	70%	This study

5.1.4 Conversion

In this step, the solar cell area is laminated and cut into pieces of the desired size. All layers in the OPV-C cell are added in a pattern on the right and left side of the substrate. In the lamination step, the substrate is folded lengthwise and sealed, before it is cut into appropriately sized pieces, forming the final solar cell. This means that the final area of the solar cell, before cutting, is half of the processed area. Excess PET substrate that has been cut off is assumed to be discarded to hazardous waste treatment. In this process, 30% of the processed area is assumed to be scrapped, giving a yield of 70%. This yield is used for calculating the impact of the solar cell based on the functional unit of 1 m^2 active area, however, it is not used for comparison with other OPV cells, as previous LCAs have not mentioned scrap rates in their analysis. The lamination step in this study differs from the lamination in other studies, as the substrate in other studies is not folded lengthwise. Nevertheless, data from Espinosa et al. (2012b) is used, stating that the lamination process requires 4.1 Wh per m^2 processed area, see Table 6.

Table 6. Energy requirements for lamination. The chosen proxy data for this study are taken from Espinosa et al. (2012b) (within thick lines).

Lamination	
Energy per 1 m^2 (Wh)	Source
3.89	(Espinosa et al., 2013)
4.31	(Espinosa et al., 2012a)
4.10	(Espinosa et al., 2012b)
6.68	(Espinosa, García-Valverde, Urbina, et al., 2011)

5.1.5 Testing

After manufacturing, the finished solar cells are tested to ensure their functionality. This step is also called characterisation (not to be confused with the characterisation step of life cycle impact assessment – see Section 2). Four LCA studies mention testing as part of the analysis, however, none includes the testing process in the inventory (Espinosa et al., 2011, 2013; Espinosa et al., 2012a; Espinosa et al., 2012b). For this reason, and lack of specific information regarding the procedure, environmental impacts related to this process was not considered in this study. To conclude, all inputs and outputs to the foreground system are provided in Table 7. Input and output materials will be described in more detail in Section 5.2.

Table 7. Inputs and outputs for roll-to-roll manufacturing of 1 m^2 processed OPV-C area. For confidentiality reasons, some materials and amounts cannot be specified. n.d. = not disclosed.

Inputs			Unit
	PET Barrier Substrate	72	g
	Graphite	0.98	g
	Carbon black	0.37	g
	Dipropylene glycol monomethyl ether	3.3	g
	Solvent	n.d.	
	Surfactant	n.d.	
	PEDOT:PSS (solution)	5.9	g
	H_2O	5.6	g
	Isopropanol	10	g
	ZnO	0.12	g
	Solvent	n.d.	
	P3HT	0.19	g
	PCBM	0.19	g
	Xylene	7.7	g
	P3HT	0.19	g
	PCBM	0.19	g
	Xylene	7.7	g
	Electricity	2.5	kWh
Outputs			
Liquid waste	Graphite	0.10	g
	Carbon black	0.04	g
	Dipropylene glycol monomethyl ether	0.33	g
	Solvent	n.d.	
	Surfactant	n.d.	
	PEDOT:PSS (solution)	0.59	g
	H_2O	0.56	g
	Isopropanol	1.0	g
	ZnO	0.01	g
	Solvent	0.37	g
	P3HT	0.02	g
	PCBM	0.02	g
	Xylene	0.77	g
	P3HT	0.02	g
	PCBM	0.02	g
	Xylene	0.77	g

Emissions to air	Dipropylene glycol monomethyl ether	3.0	g
	Solvent	n.d.	
	H_2O	10	g
	Isopropanol	9.2	g
	Solvent	n.d.	
	Xylene	13.88621	g

5.2 Materials Manufacturing

In this section, the background processes for the materials used in the solar cells are explained in more detail. In Table 8, the inventory data sources for each ingoing material is presented. As can be seen, the majority of inputs have inventory data in Ecoinvent ("ecoinvent 3.5 – ecoinvent," 2018; Wernet et al., 2016). For inputs that are not available in Ecoinvent, data from the scientific literature have been gathered.

Table 8. Life cycle inventory data sources for all input materials to the foreground system. For confidentiality reasons, some materials and amounts cannot be specified.

Layers and materials	Comment	LCI data source
PET Substrate		
PET Substrate		Ecoinvent
Metal oxide	Material production omitted	(Espinosa et al., 2012a)
Non-halogenated Resin	Material production omitted	(Espinosa et al., 2012a)
Carbon ink		
Graphite		Ecoinvent
Carbon black		Ecoinvent
Solvent	Proxy used for all these carbon ink solvents: Dipropylene glycol monomethyl ether (Espinosa, Laurent, dos Reis Benatto, Hösel, & Krebs, 2015)	Ecoinvent
Solvent		
Solvent		
Solvent		
PEDOT-layer		
Solvent		Ecoinvent
Surfactant		Ecoinvent
PEDOT:PSS		(Roes, Alsema, Blok, & Patel, 2009)
H_2O	Mixed with PEDOT:PSS	Ecoinvent
H_2O	Mixed with isopropanol	Ecoinvent
Isopropanol		Ecoinvent
ETL		
Zinc oxide	Generic zinc oxide used as proxy	Ecoinvent
Solvent		
AL 1 & 2		
P3HT		(Anctil, 2011; García-Valverde et al., 2010)
PCBM		(Anctil, 2011)
Xylene		Ecoinvent

For an overview of input materials and their mass percentage, see Table 9. Note that this represents the mass of input materials per reference flow (1 m^2 processed cell area), but as explained in the previous section, all solvents evaporate during the drying processes and are not present in the final cell.

Table 9. Description and mass percentage of input materials per 1 m^2 processed area. For confidentiality reasons, some materials and amounts cannot be specified. n.d. = not disclosed.

Layer	Materials	Description	Mass (g)	Mass percentage
PET	PET Substrate	Plastic film	72	62.99%
	Metal Oxide	Barrier material	-	-
	Non-halogenated resin	Epoxy	-	-
Carbon Electrodes	Graphite	Carbon	0.88	0.77%
	Carbon black	Carbon	0.34	0.29%
	Dipropylene glycol monomethyl ether	Solvent	3.0	2.62%
PEDOT-layer	Solvent	Solvent	n.d.	n.d.
	Surfactant	Surfactant	n.d.	n.d.
	PEDOT:PSS	Polymer	5.3	4.65%
	H_2O	Solvent	5.0	4.42%
	Isopropanol	Solvent	9.2	8.11%
ETL	Zinc oxide	Metal oxide, powder	0.11	0.09%
	Solvent	Solvent	n.d.	n.d.
AL 1 & 2	P3HT	Polymer	0.34	0.29%
	PCBM	Fullerene	0.34	0.29%
	Xylene	Solvent	14	12.19%

5.2.1 PET Barrier Substrate

The PET substrate is a barrier film with a thickness of approximately 50 μm. The PET substrate has a barrier of metal oxide and non-halogenated resin According to the data sheet provided by the supplier, 90-98% of the mass is PET film, whereas the barrier materials, metal oxides and non-halogenated resin, are 1-5% respectively. LCI data for the PET substrate manufacturing process, including PET granulate production and film extrusion, is found in Ecoinvent (Wernet et al., 2016). The specifics of the barrier materials are a trade secret, complicating the procedure of finding reliable inventory data. What is known is that the barrier is added to the PET substrate through sputtering. Sputtering is a deposition technique where particles of metals are sprayed on a surface in a vacuum environment. It is an energy-intensive method, mainly because of the energy required to create vacuum. No information has been found regarding the specifics of the sputtering process in this case, other than that a metal oxide has been sputtered on one side of the barrier.

Sputtering processes are common in OPV manufacturing. However, it is mostly used for the deposition of ITO electrodes. One study where sputtering has been used for a barrier was made by Espinosa et al. (2012a). In this study, a Kapton polyimide substrate is sputtered with aluminium (Al) and chromium (Cr). For the sputtering process, the substrate roll is loaded into a chamber that is pumped overnight (12 h) to create a vacuum. The pumping process uses 88.53

MJ EPE (equivalent primary energy). During the sputtering process, the substrate is rolled through the chamber while metal particles are sputtered onto it. In the example of Espinosa et al. (2012a), the substrate is sputtered twice and all energy used is electrical energy. The material manufacturing has negligible impact (less than 1%) on the embedded energy use for the sputtering process (Espinosa et al., 2012a). This indicates that neglecting the manufacturing of the unknown barrier materials in this study will not have a significant impact on the results. It is worth noting that the use of Kapton in place of PET was to ensure thermal stability during the laboratory-scale production, however, the authors advise other producers to use PET for the substrate material as Kapton is not economically viable for large-scale production. For this reason, the rest of their analysis assumes PET to be the substrate material.

In addition to the electricity for sputtering, argon production will be included in this study. Inventory for argon production is found in Ecoinvent. However, the result on CED in Ecoinvent differs significantly from literature data. In Espinosa et al. (2012a), the production of 0.1 N m^3 argon is said to require 65 MJ primary energy. This volume translates to 0.1784 kg argon, which according to Ecoinvent data uses less than 7 MJ. The data from Espinosa et al. (2012a) origins from an article by largely the same authors from 2010, where argon production data are collected from a manufacturer and the energy requirements are estimated (García-Valverde et al., 2010). In the later article, Espinosa et al. (2012a) consider their data certainty to be very good. For this reason, and in order to make a conservative estimate, the data for the CED of argon production found in the literature is used in this study. This means that the entire sputtering process data from Espinosa et al. (2012a) is applied directly in this study.

The total energy requirements for the sputtering process, including pumping, sputtering and argon production, is 320 MJ EPE (primary energy), which translates to approximately 112 MJ direct input of electricity. This is data was gathered by Espinosa et al. (2012a) directly from a manufacturer. Another study that looks into a sputtering process is García-Valverde et al. (2010). In this study, ITO is sputtered on a glass substrate, and the electrical energy input for the sputtering process is 59 MJ. This is significantly lower than the results from the study mentioned above, however, as the sputtering process in Espinosa et al. (2012a) is more similar to the one being investigated in this study, 112 MJ direct input energy is used as proxy for the barrier sputtering process.

5.2.2 Carbon Electrodes

The applied carbon ink contains graphene and carbon black mixed with a set of solvents. The types of solvents and their approximate ratios are given by the product data sheet, but the carbon content is a trade secret and the solvents cannot be disclosed due to confidentiality reasons.

Due to the fact that complete inventory data for the carbon ink is not possible to find, carbon ink used in Krebs et al. (2015) is used as a proxy. The material composition for the carbon ink proxy was found in the supporting information of Krebs et al. (2015), but was originally from (Espinosa et al., 2015), see Table 10. The composition differs by using graphite instead of graphene as well as using a different solvent. Inventory for all these ingoing materials can be found in Ecoinvent.

Table 10. Material composition for1 kg of carbon ink. Gathered from Espinosa et al. (2015).

Carbon Ink	Mass percentage
Graphite	21%
Carbon Black	8%
Dipropylene glycol monomethyl ether	71%

5.2.3 PEDOT-layer

PEDOT:PSS is a polymer created from two components: PEDOT, poly(3,4-ethylenedioxythiophene), and PSS, polystyrene sulfonate (Groenendaal, Jonas, Freitag, Pielartzik, & Reynolds, 2000). It was developed in the 1980s and is widely used in OPV due to its high conductivity and transparency (Günes & Sariciftci, 2017). PEDOT is a conjugated polymer based on polythiophene. However, it is not water-soluble. This problem is circumvented by using the water-soluble polyelectrolyte PSS as a dopant. Thereby, a highly conductive, transparent polymer with good film-forming properties is created. The production of PEDOT:PSS is done in three steps: first, production of EDOT (ethylenedioxythiophene), which is a monomer, then production of PSS, third, EDOT it polymerized with PSS to create PEDOT:PSS (Roes et al., 2009). This is done using standard oxidative chemical or electrochemical polymerization methods (García-Valverde et al., 2010). Inventory data for PEDOT:PSS is shown in Table 11. The ingoing PEDOT:PSS is mixed with water as solvent. The mass percentage of PEDOT:PSS in this mixture is 1.3%. Thus, the amount of PEDOT:PSS in the final product is less than a gram per square metre processed area. Inventory data for PEDOT:PSS is presented in Table 11.

Table 11. Inventory data for PEDOT:PSS for 1 m^2 processed area (Roes et al., 2009).

PEDOT:PSS			
	Name	Amount	Unit
Output	PEDOT:PSS	0.00589	g
Material Inputs	Propene	0.00099	g
	Ethene	0.00132	g
	Acetic acid	0.00283	g
	Sodium sulphate	0.00334	g
	Dichloroethane	0.00144	g
	Polystyrene	0.00214	g
	Sulfuric acid	0.00412	g
	Water	0.00581	g
Process inputs	Electricity	5.26	Wh el.
	Steam	0.04015	g

In addition to PEDOT:PSS, this layer also contains surfactants and solvents. These cannot be displayed due to confidentiality reasons.

5.2.4 Electron Transport Layer

The ETL layer is made from a zinc oxide and a solvent. The exact type of zinc oxide and solvent is not disclosed due to confidentiality, instead, a generic zinc oxide from Ecoinvent is used for the inventory data. For the solvent, inventory data are also found in Ecoinvent.

5.2.5 Active Layer 1 & 2

The active layer is made from poly(3-hexylthiophene) (P3HT), which is a polymer, and phenyl-C61-butyric acid methyl ester ($PC_{60}BM$, or PCBM), which is a fullerene derivative. In more detail, P3HT is a semiconducting polymer which acts as the electron donor, whereas PCBM acts as the acceptor. The inventory data for P3HT was initially retrieved from Anctil (2011).

This inventory contains over 50 separate inputs, some of which are not available in Ecoinvent. A less extensive inventory list for P3HT is found in García-Valverde et al. (2010). According to this study, the ingoing materials are bromine, thiophene, hexane and water for cooling. However, inventory data for thiophene, which makes up almost half of the inputs, is not found in Ecoinvent. For the scope of this study and due to the fact that P3HT represents less than 0.1% of embodied energy in previous LCA studies of OPVs (Espinosa et al., 2012a; Espinosa et al., 2013), it is, aside from CED calculation, excluded from the impact assessment due to the unavailability of data. The cumulative energy demand for 1 kg P3HT is 1809.52 MJ (Espinosa et al., 2012a).

Fullerenes are spherical molecules made of carbon (Figure 8). Different fullerenes have slightly different shapes and can be manipulated for different purposes. They are, amongst other things, useful for electrical technology (Ungvarsky, 2019). By adding a molecule on top of the fullerene, fullerene derivates, such as PCBM, can be synthesized. Although fullerenes account for less than 1% of the final weight of an OPV cell, they can comprise up to 19% of the embodied energy (Kim & Fthenakis, 2013). Fullerenes can differ both in their round shape, and have different molecules attached on the outside of the sphere. The fullerene derivative in the solar cell of this study is $PC_{60}BM$, which means that the added chemical is methyl 4 benzoylbutyrate p-tosylhydrazone, see Figure 8 (Anctil et al., 2011).

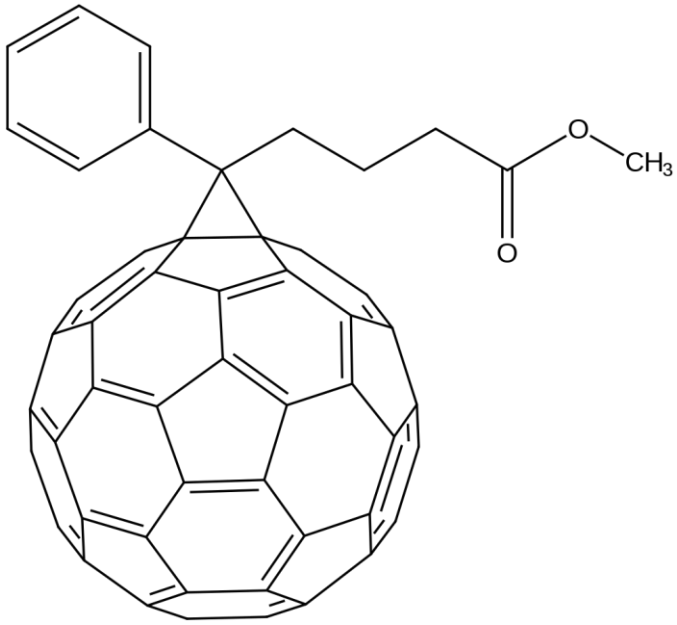

Figure 8. $PC_{60}BM$ molecule (Nothingserious, 2016).

Anctil, Babbitt, Raffaelle, & Landi (2011) have assessed the material and energy intensity of fullerene production. In their study, inventory and embodied energy of two types fullerene production can be found: pyrolysis and plasma. However, they do not apply impact categories other than energy use due to uncertainty regarding direct emissions in the pyrolysis process. This makes it complicated to apply impact categories on fullerene production in this study. Different studies show different results regarding the CED of fullerenes. According to Anctil et al. (2011), previous studies underestimate the CED of fullerenes by as much as 48%.

As mentioned above, there are two different production methods available for producing fullerene C60: pyrolysis and plasma (Anctil et al., 2011). Plasma methods have been considered

more environmentally friendly as they do not generate direct gas emissions during the process. However, plasma methods require significantly more energy. Thus, it is assumed that pyrolysis is used to produce C60. In the pyrolysis process, either toluene or tetralin (1,2,3,4-tetra-hydronaphthalene) can be used as feedstock. Using tetralin leads to less gaseous carbon emissions compared to toluene. The amount and nature of the emissions depend on conditions such as temperature profile of the reactor, precursor and oxygen ratio.

Despite the fact that the study by Anctil et al. (2011) only focuses on embodied energy and inventories for fullerene production, efforts are made in this study to derive other inventory data than energy use. However, due to the complexity of the material and lack of information regarding direct process emissions, the impact assessment will be an estimation. For the inventory of C60 PCBM, see Table 12. The biggest contributor to the CED is tetralin, which is a hydrocarbon. The tetralin in 1 kg C60 PCBM represents 33.7 GJ, which is 37.4% of the total CED. Tetralin is made from naphthalene, which in turn is made from coal tar-products. The ingoing products in tetralin production are tar, heat, steam and electricity (Anctil, Babbitt, Raffaelle, & Landi, n.d.). Although tetralin is not available in Ecoinvent, the raw materials such as tar and steam are. However, when the inputs are allocated by weight, it results in a total CED of 57 MJ per kilo tetralin, which is a little low compared to the 79 MJ presented by Anctil et al (2011).

Other studies have results of the embodied energy of PCBM C60 around 7.7 MJ/kg (García-Valverde et al., 2010). This is considerably lower than Anctil et al. (2011) showing an embodied energy of 65 GJ for PCBM C60. As mentioned above, the differences are likely due to the larger scope in the study by Anctil et al. (2011).

Inventory data for the chemical methyl 4 benzoylbutyrate p-tosylhydrazone has not been found. This is the molecule that is added to the spherical fullerene, making it PCBM, see Figure 8 above. Its predecessors also lack inventory data in Ecoinvent, as it is a relatively exotic molecule. For this reason, it is excluded from the study.

Table 12. Input for PCBM C60 for 1 m^2 processed area (Anctil et al., 2011).

PCBM C60, 99.9%			
	Name	Amount	Unit
Output	PCBM C60	0.19	g
Inputs	Toluene	0.95	g
	Tetralin	52	g
	Pyridine	7.8	g
	Methanol	2.2	g
	o-xylene	18	g
	O-dichlorobenzene	1.23	g
	Methyl 4 benzoylbutyrate p-tosylhydrazone	0.39	g
	Nitrogen, gas cylinder	3.7	g
	Oxygen, gas cylinder	44	g
	Train	0.19	t*km
	Lorry, 16t,	0.05	t*km
	Steam	660	g
	Electricity	0.13	kWh

5.3 Use Phase

The solar cells can be used in many different applications. However, this study focuses on small scale indoor applications such as powering electronic price tags, displays or alarms. For indoor applications, the solar cells will not be able to substitute electrical power from the grid, but they essentially use electric power. As long as the indoor lights are turned on regardless of the OPV-C cell being in place or not, there are no direct inputs related to the use phase of the solar cells. However, there is a risk that lights are being kept on in order to keep indoor-light powered devices powered. Contributing to more electrical power-use would have a negative impact on the life cycle of the cell, although this contribution would be complicated to assess. This means that the OPV-C cell needs to be placed in an area where light is turned on enough hours per day for the OPV-C to be able to supply energy to its devices. However, this could also become a technological lock-in, thus becoming a prevention towards energy savings, due to the fact that the OPV-C-powered devices will not function if the lights are turned off.

5.4 End of Life

At the end of solar cells' lifetime, which is expected to be after 10 years indoor use, they are assumed to be sent to hazardous waste treatment. This is a rather pessimistic scenario, considering that no energy recovery from incineration is granted the solar cell. Another possibility could be that the largely organic solar cells would become incinerated, resulting in heat and electricity that might be credited to the cell through substitution, thus lowering its environmental impacts. However, the feasibility of OPV-C combustion, as well as emissions and waste thereof, are beyond the scope of this study to investigate.

5.5 Assessing Future Large Scale Application

In this section, the equations used to assess the future large scale application of OPV-C are presented. This is based on a hypothetical scenario for the future, not on current applications. It is assumed that this type of solar cell can be used for large-scale energy production in environments rich in sunlight.

5.5.1 Calculating Area Producing 1 kWh

The kWh energy produced by a solar cell is based on assumptions regarding total energy production during its lifetime. The area of solar cell needed to produce 1 kWh during its 10 year lifetime is calculated according to equation 1 (Lunardi, Ho-Baille, Alvarez-Gaitan, Moore, & Corkish, 2017):

$$A = \frac{\varepsilon}{\eta \cdot I \cdot y \cdot PR} \qquad \text{Equation 1}$$

where A is the area, ε is the energy produced (in this case 1 kWh), η is the power conversion efficiency, I is the insolation in MJ/m^2/year, y is the guaranteed lifetime in years and PR is the performance ratio. The performance ratio is a quality measure that describes the ratio between the theoretical and the actual energy output of the solar cell or solar plant. In the Methodology Guidelines on Life Cycle Assessment of Photovoltaic Electricity, it is recommended to use a PR of 0.75 for rooftop applications and 0.8 for ground mounted solar cells (Raugei et al., 2011). Most of the LCAs on OPV that have been referred to in this study have used a PR of between 0.75 and 0.85 (Espinosa et al., 2012a; Espinosa et al., 2013; M. P. Tsang, Sonnemann, & Bassani, 2016; M. Tsang & Sonnemann, 2016; M. Tsang, Sonnemann, & Bassani, 2015). In this analysis, a PR of 0.8 is applied, thus assuming ground-mounted cells.

5.5.2 Calculating Energy Payback Time

The following formula is used to calculate the EPBT (M. Tsang & Sonnemann, 2016):

$$EPBT = \frac{CED}{E_g} \qquad \text{Equation 2}$$

where E_g is defined as:

$$E = \frac{I \cdot PR \cdot \eta}{X} \qquad \text{Equation 3}$$

and where I is the insolation in MJ/m^2/year, PR is the performance ratio, η is the power conversion efficiency and X is the electrical conversion efficiency, which is here assumed to be 0.35, as used by similar studies (Espinosa et al., 2012b; Espinosa et al., 2013).

5.5.3 Calculating Energy Return Factor

The energy return factor (ERF) is an expression of how much energy is saved per unit of invested energy (Espinosa et al., 2012a).

The ERF is calculated with the following equation:

$$ERF = \frac{L}{EPBT} \qquad \text{Equation 4}$$

This is the lifetime L of the PV module in years divided by the EPBT as described in Equation 2.

6 Results

In this section, the results from the life cycle impact assessment and the future large scale application scenario are presented.

6.1 Life Cycle Impact Assessment Results

The inventory section has been described using the reference flow of 1 m^2 processes area. This is partly because it is an easily comprehensible unit but also because it carries relevance when describing manufacturing processes and inputs. This is also the unit used in many other LCAs on OPV. In this section, however, the functional unit of 1 m^2 *active* area is used. In addition to allocating all impact to the active area, 30% loss is applied in the conversion step of the manufacturing process, see Section 5.1.4.

For all impact categories, aside from CED, the results depend on what electricity mix is assumed to be used. The baseline scenario for all production aside from the PET sputtering is a German electricity mix. As the sputtering has the biggest impact by far due to its high energy use, it is presented with two different electricity mixes as input, Swedish and German.

6.1.1 Cumulative Energy Demand

The CED for producing 1 m^2 active area of OPV-C is 900 MJ. Looking closer at the foreground and the background system, one can see that the background system makes up 95% of the energy required to produce the OPV-C, see Figure 9.

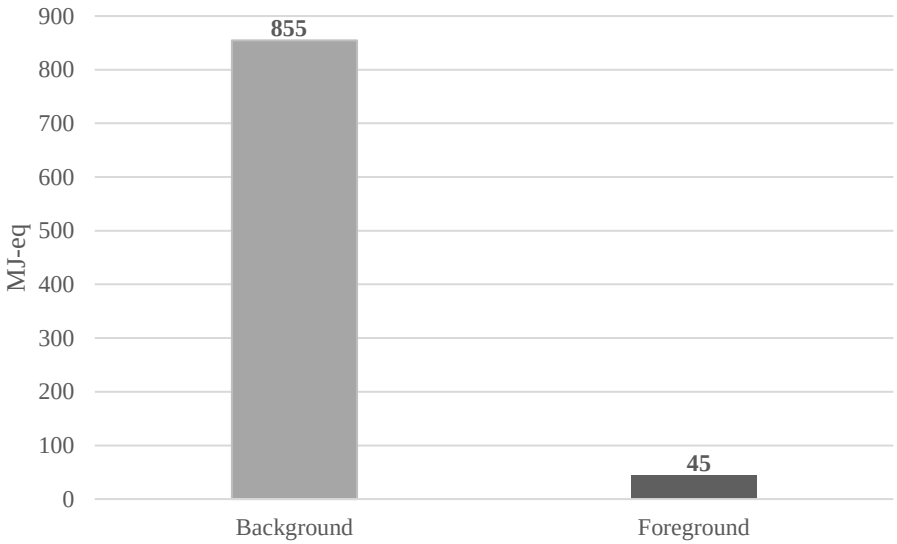

Figure 9. Cumulative energy demand for the foreground and background system, respectively.

In Figure 10, the CED is presented for each main process in the solar cell's life cycle. It is clear that the manufacturing of the PET barrier substrate has, by far, the largest impact, making up almost 90% of the CED.

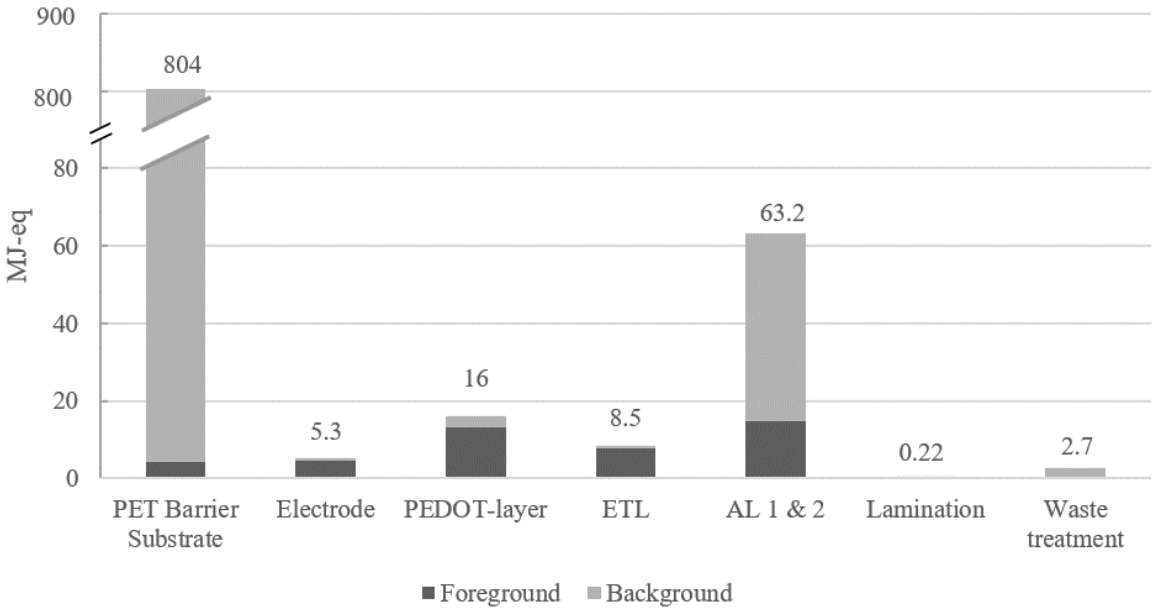

Figure 10. Cumulative Energy Demand (CED) for all layers including their materials and processing steps. The foreground system (in blue) includes all R2R (roll-to-roll) processes and is only electric energy. The background processes (in orange) include raw material extraction, materials manufacturing and waste treatment.

Regarding the R2R processes, the drying of the PEDOT-layer is the most energy intensive process. This is expected, as this layer consists of more ink than the others, and therefore requires more heat to evaporate the solvents. The drying processes are also the most energy-intense overall. It should however be remembered that this information is derived from proxy data from similar studies, and it is therefore an indication rather than a representation of the actual system.

When taking a closer look at the PET barrier substrate production, it is clear that the sputtering process constitutes the largest share of the required energy, see figure 11. One should keep in mind that also the argon production is a part of the sputtering process, and only granulate production and extrusion are processes related to the plastic film manufacturing itself. As mentioned in Section 5, the barrier material production is excluded from the analysis. It is not believed to have a significant impact compared to the sputtering process itself.

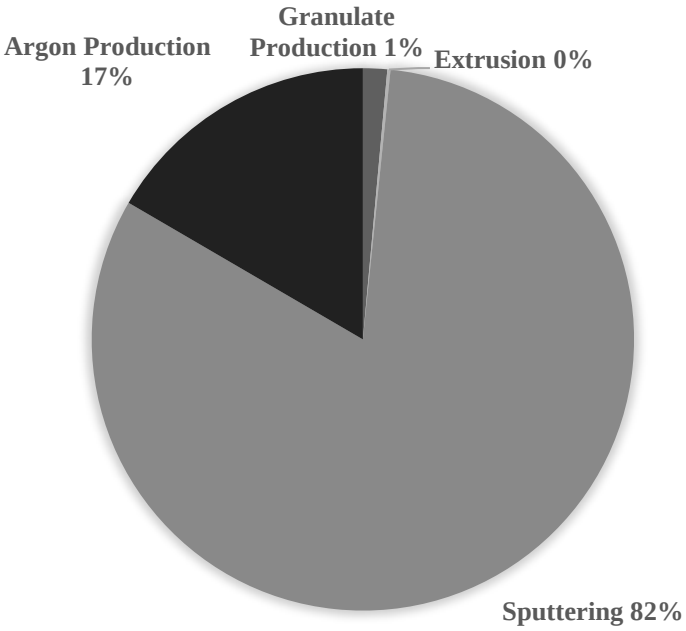

Figure 11. Share of cumulative energy demand for production of PET barrier substrate.

Regarding the photoactive layers, AL 1 and AL 2 are more energy intensive than the others. As these layers were included with the same input materials and ratios in this study, they are combined in Figure 12. Breaking the input materials down, one can see that the PCBM makes up the absolute majority of the CED.

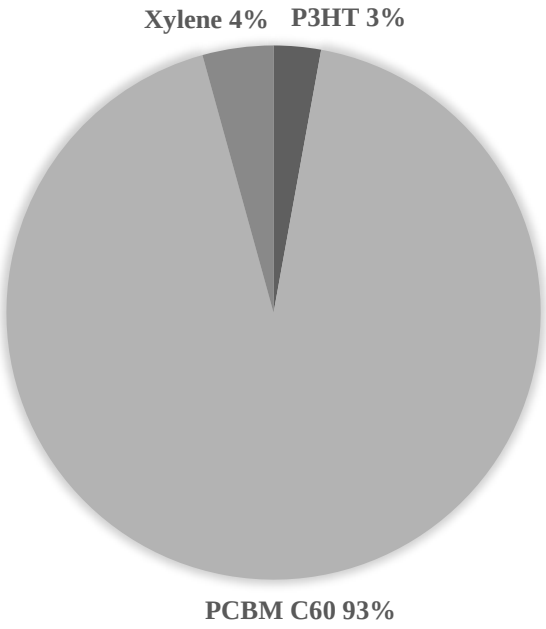

Figure 12. Share of cumulative energy demand of background processes for the active layers, AL 1 and AL 2.

6.1.2 Climate Change 100 years

Emissions of greenhouse gases contribute to global warming, as they increase the radioactive forcing in the atmosphere. Because energy production tends to generate carbon emissions, the

CED often correlates rather well with the impact on climate change. As can be seen in Figure 13, the foreground processes have a much smaller impact on climate change compared to the background processes. This is because the manufacturing of the OPV-C cell takes place in Sweden, where the electricity mix has a comparably small carbon footprint. In Figure 14 and 15, as well as the subsequent sections, the foreground system is presented as its own bar named R2R processes, whereas all other bars are part of the background system. As the PET barrier substrate is the biggest contributor in all impact categories, it is presented with two different electricity mixes, whereas all other layers and processes are presented as a baseline scenario with the same assumptions that are established in the beginning of this section, 6.1.

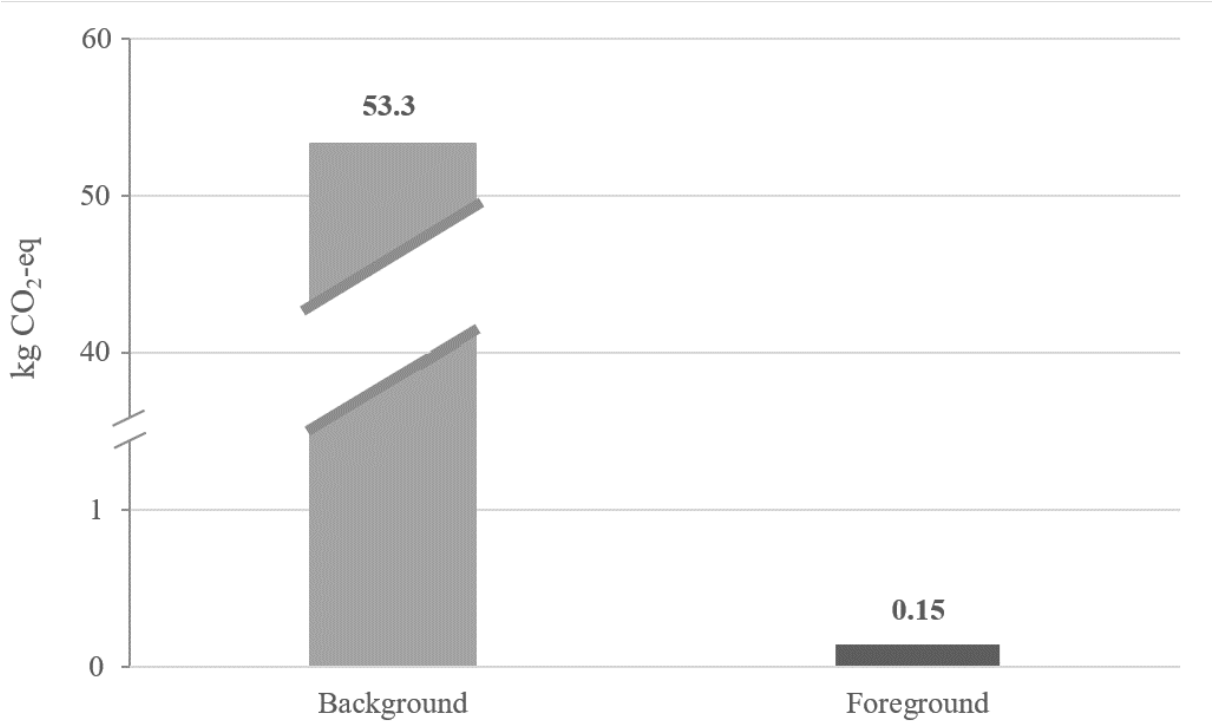

Figure 13. Climate change over 100 years for the background and foreground system, measured in CO_2-eqvivalents. German electricity mix assumed.

Looking more closely into the materials in Figure 14, it is again the PET barrier substrate that has the largest impact. As was shown in Section 6.1.1 the majority of the energy in the PET substrate production is related to the sputtering process, which only has electric energy inputs, meaning that the electricity mix used plays a vital role in the total climate change impact of not only the PET barrier substrate, but also the entire solar cell. If a Swedish electricity mix was to be used for the sputtering process instead of the German mix, the climate change impact of the PET barrier substrate would be 93% lower, see Figure 14.

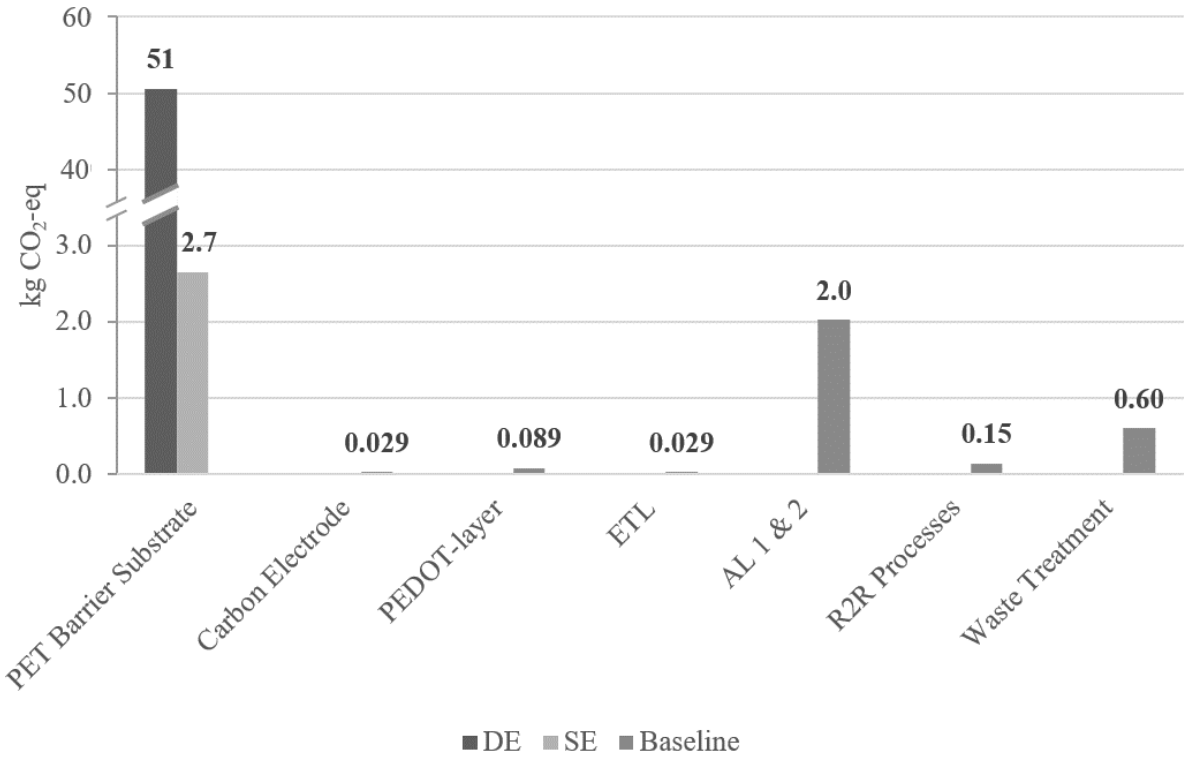

Figure 14. Climate change impact, comparing a Swedish electricity mix with a German electricity mix for the sputtering process of the PET barrier substrate. The baseline represents the data from the inventory, mainly gathered directly from EcoInvent or proxy data. In the few cases where electricity is part of the baseline scenario, a German electricity mix is assumed.

Looking more closely at the case where a Swedish electricity mix is used in the sputtering and argon production process, one can see that the PET barrier substrate still has the largest impact on climate change, but it is only slightly higher than for the two active layers. Thus, in this scenario, the active layer are relatively large contributors to climate change for the OPV-C.

6.1.3 Freshwater Ecotoxicity

As can be seen in Figure 15, the PET barrier substrate contributes the most to freshwater ecotoxicity as well. Changing the electricity mix from German to Swedish for the sputtering process makes a large difference in this category but the PET substrate is nevertheless the largest contributor.

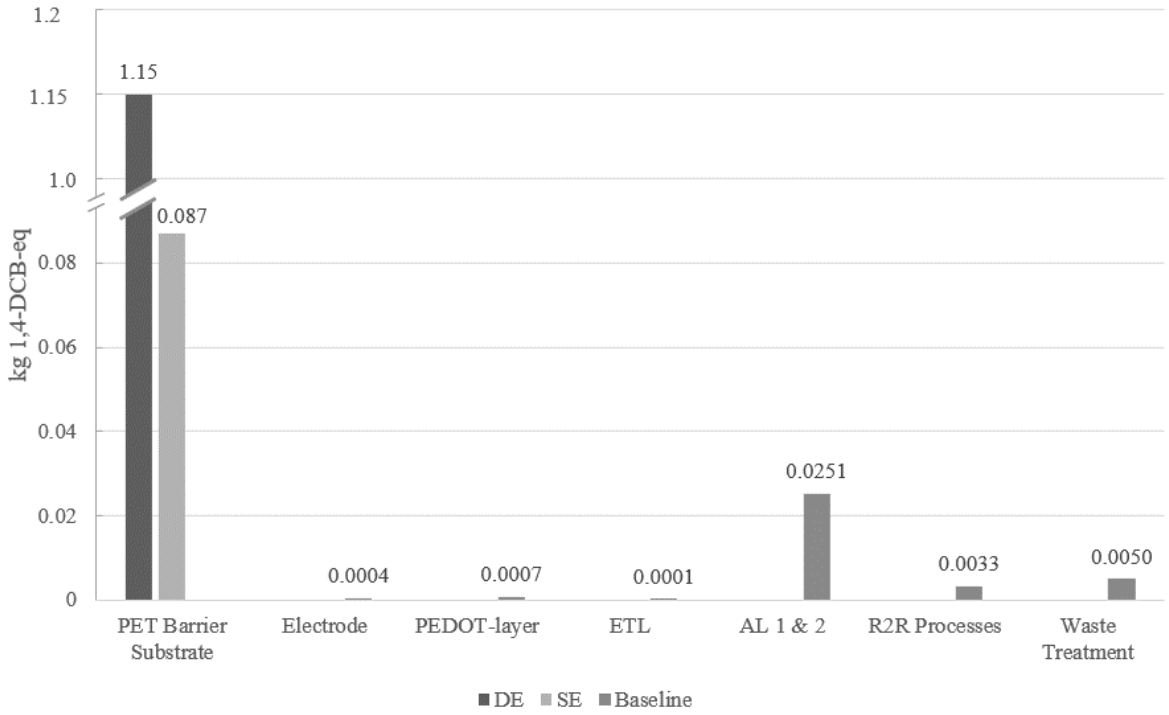

Figure 15. Freshwater ecotoxicity, comparing a Swedish electricity mix with a German electricity mix for the sputtering process of the PET barrier substrate.

6.1.4 Freshwater Eutrophication

Regarding freshwater eutrophication, the impact from the German electricity mix is again very large, see Figure 16.

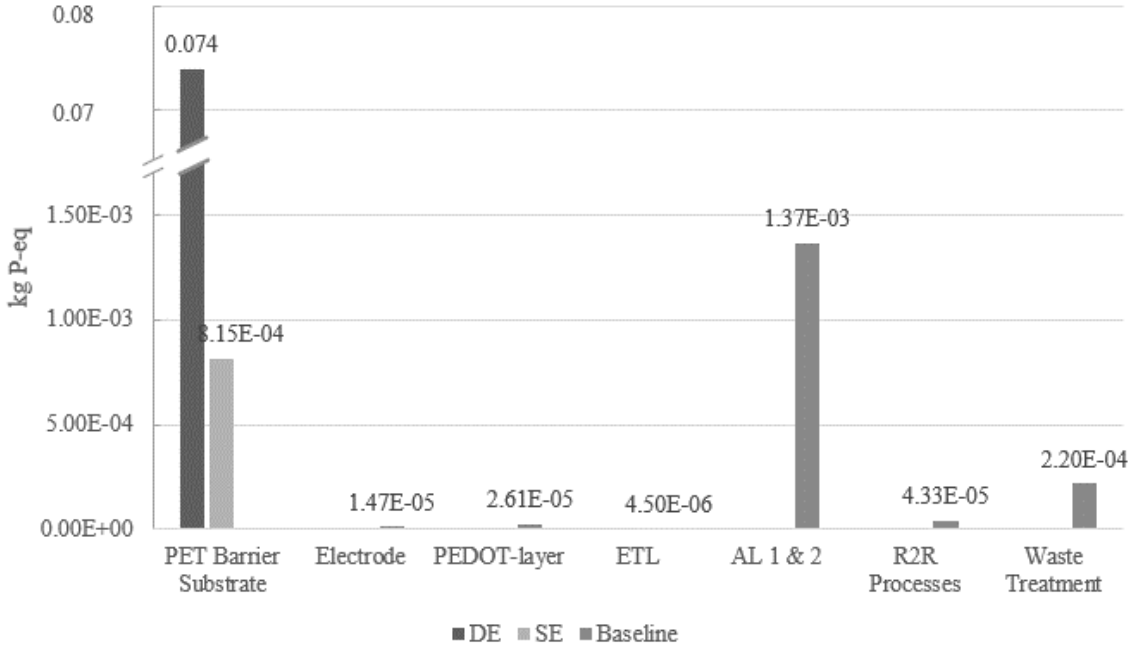

Figure 16. Freshwater eutrophication, comparing a Swedish electricity mix with a German electricity mix for the sputtering process of the PET barrier substrate.

Looking at the same categories with a Swedish electricity mix for the sputtering process, the two active layers have a larger contribution than the PET barrier.

6.1.5 Terrestrial Ecotoxicity

For this impact category, the differences between a Swedish electricity mix and a German electricity mix is significantly lower than in the others. Although the PET barrier substrate is again the largest contributor, it is also worth noting that the PEDOT- layer has a larger impact than the active layers for this category. For the PEDOT- layer, it is not the PEDOT:PSS solution that creates the large impact in this category, but the surfactant, see Figure 17 and 18. Due to lack of data for the authentic surfactant, a generic surfactant was used for the impact assessment, see Section 5.2.3.

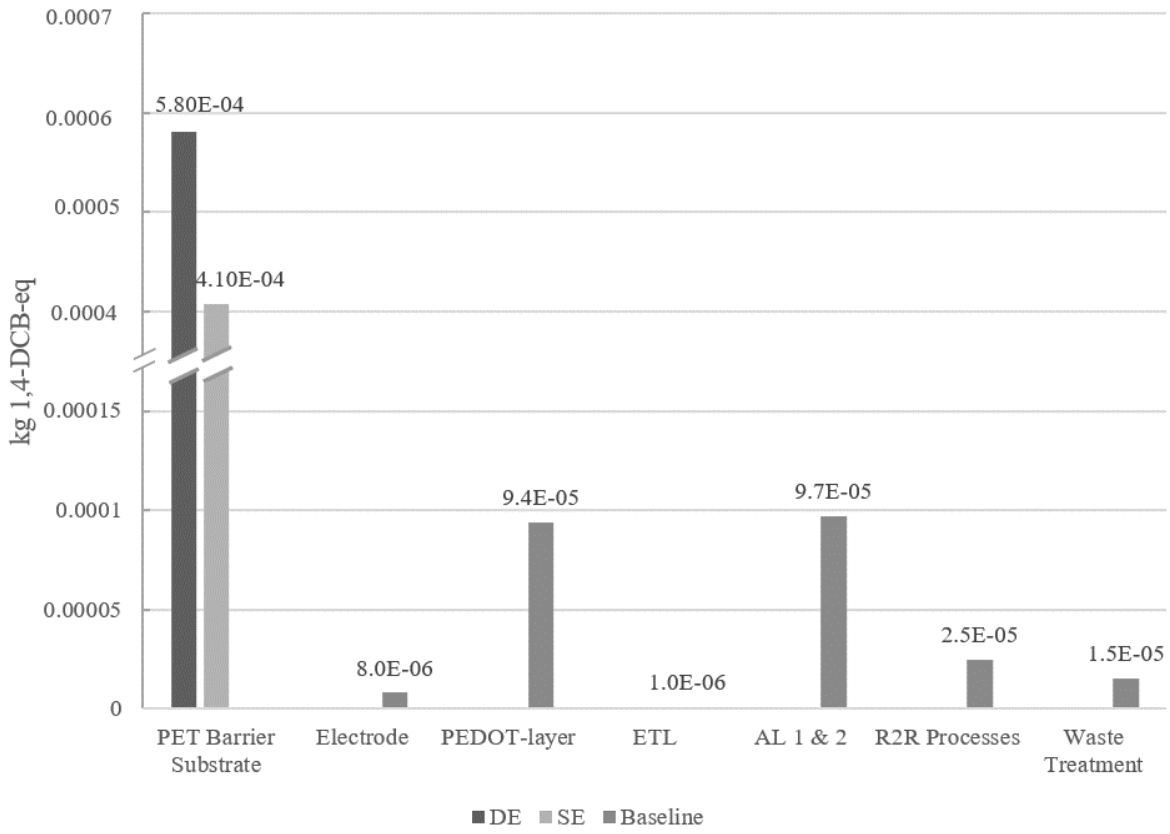

Figure 17. Terrestrial ecotoxicity comparing a Swedish electricity mix with a German electricity mix for the sputtering process of the PET barrier substrate.

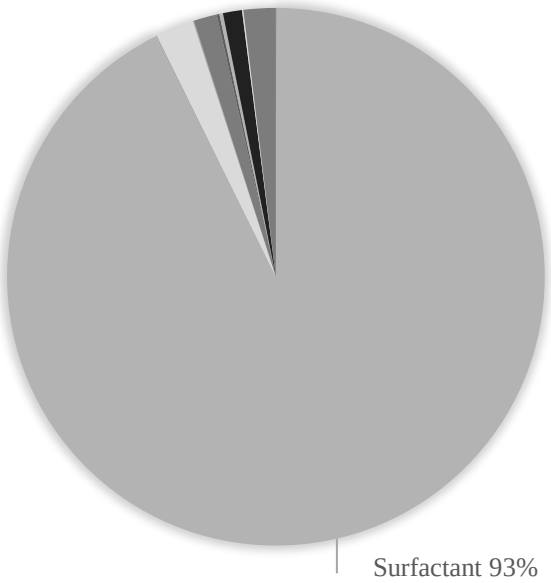

Figure 18. Share of impact on terrestrial ecotoxicity of the surfactant in the PEDOT- layer.

6.1.6 Water Depletion

As shown by Figure 19, the electricity intensive processes show the largest impact on water depletion, meaning that the PET barrier substrate again is main contributor. However, the importance of electricity also shows in the foreground system, as the R2R processes have the second largest impact overall.

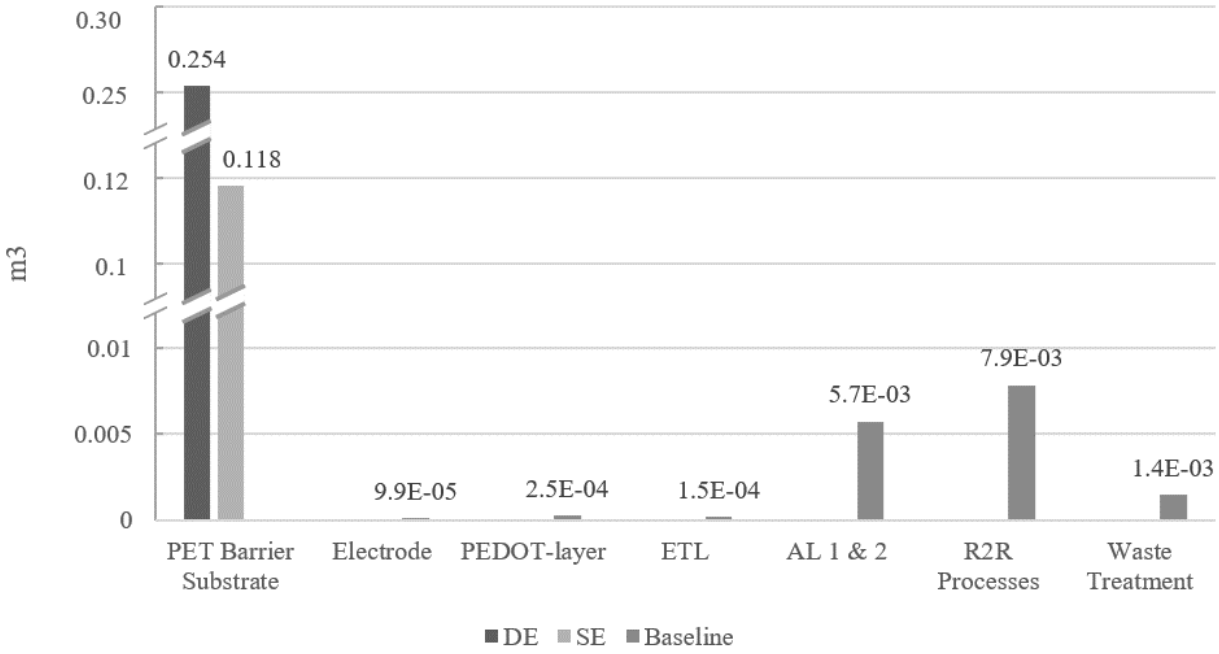

Figure 19. Water depletion, comparing a Swedish electricity mix with a German electricity mix for the sputtering process of the PET barrier substrate.

6.2 Future Large Scale Application Results

In this section, the results regarding electricity production, EPBT and ERF are presented. The previously assumed production yield of 70%, where 30% of the processed area was scrapped in the conversion step, will here be neglected, and the yield is assumed to be 100%. This is because a future production yield is unknown, but it could be as high as 99%, and a yield of 95-100% has been assumed in other studies (Espinosa & Krebs, 2014; Hengevoss et al., 2016). However, a 10% loss of ingoing ink to the processes was still assumed.

The OPV-C solar cells have a guaranteed indoor lifetime of 10 years and this is assumed to apply at large scale as well. Furthermore, the OPV-C cells have an estimated power conversion efficiency (PCE, or just efficiency) of 5%, but a future goal is to reach 10%. An efficiency of 5% generates 50 W_p/m^2. W_p is a standard way of comparing solar cells, where standard conditions are established (Energuide, 2019). Unless standards conditions are established, it would be a complicated task to quantify the energy output, as it constantly varies with the conditions. The main condition is of course the insolation (incoming solar light), but also temperature plays a role in the electric output of a solar cell, as warmer temperatures decreases the efficiency.

6.2.1 Producing 1 kWh

Equation 1 presented in Section 5.5 is used to calculate the area required to produce 1 kWh of electricity for a future large scale application of the OPV-C cells. This information can be used for assessing the environmental impact per kWh in a future scenario.

Aside from the standard watt-peak conditions, a common assumption is that a solar cell receives 1700 kWh/m^2/year of insolation. This assumption has been made in several other OPV LCAs and is thus good for creating comparable results (Espinosa et al., 2012a; Espinosa et al., 2013; Raugei et al., 2011; M. Tsang & Sonnemann, 2016). Based on these assumptions, presented in Table 13, the area needed to produce 1 kWh during the solar cell lifetime in world average solar conditions is almost 15 cm^2.

Table 13. Inputs and output for Equation 1.

Energy Output (kWh)	Efficiency (PCE)	Lifetime (years)	Performance ratio	Area (cm^2)
1	5%	10	0.8	14.7

If the cell efficiency were to be 10% instead of 5%, the area needed to produce 1 kWh under its lifetime would be exactly halved, which would also halve all environmental impacts and the CED per kWh produced.

6.2.2 Energy Payback Time and ERF

Equations 2, 3 and 4 presented in Section 5.5 are used to calculate the EPBT and the ERF. Two insolation cases are applied: one with 1300 kWh/m^2/year, which is an average for Europe and one with 1700 kWh/ m^2/year, which is an average for the world, also corresponding to a southern European country (M. P. Tsang et al., 2016). In addition, the EPBT and ERF are calculated for a device with 5% PCE and 10% PCE. In Table 14, the ERF as well as the EPBT of OPV-C is presented for these four scenarios.

Table 14. Energy payback time (EPBT) and energy return factors (ERF) of OPV-C for four different scenarios.

PCE	Insolation	EPBT (months)	ERF
5%	Average Europe, 1300 kWh/ m^2/year	20.2	6.0
10%	Average Europe, 1300 kWh/ m^2/year	10.4	11.6
5%	Southern Europe, 1700 kWh/ m^2/year	15.9	7.6
10%	Southern Europe, 1700 kWh/ m^2/year	7.9	15.1

6.2.3 Comparison

A comparison of the EPBT and the ERF from other LCA studies on OPV technologies can be found in Table 15 assuming an insolation of 1700 kWh/m^2/year. Short EPBT but low ERF indicates that the solar cells have a short lifetime.

Table 15. Comparison of energy payback time (EPBT) and energy return factor (ERF) between different OPV technologies.

Active area [%]	PCE [%]	EPBT (years)	ERF (unit)	Lifetime (years)	Source
68.10	5	1.06	14.7	15	(Espinosa et al., 2012a)
68.10	10	0.53	28.24	15	(Espinosa et al., 2012a)
85	5	0.82	18.35	15	(Espinosa et al., 2012a)
85	10	0.41	36.7	15	(Espinosa et al., 2012a)
45.53	2	0.29	50.85	5	(Espinosa et al., 2013)
45.53	2	0.33	46.07	5	(Espinosa et al., 2013)
45.53	2	0.52	28.85	5	(Espinosa et al., 2013)
40	3	0.24	5 - 10	1	(Espinosa & Krebs, 2014)
40	3	0.3	5 - 10	1	(Espinosa & Krebs, 2014)
90	5	4.00	3.75	15	(García-Valverde et al., 2010)
90	10	2.00	7.49	15	(García-Valverde et al., 2010)
100	5	0.09	-	-	(M. Tsang et al., 2015)
100	5	0.2	-	-	(M. Tsang et al., 2015)
70	5	1.32	7.56	10	This study
70	10	0.66	15.12	10	This study

As can be seen in Table 15, the EPBT of the OPV-C in this study is comparable to most other OPVs, although the more recent studies (from 2014 and 2015) tend to show lower values (<0.5 years). This is probably mainly due to the high CED of the OPV-C, coming from the energy intensity of the PET barrier substrate production. The ERF largely depends on the OPV lifetime. Lifetimes between 1 and 15 year can be found in the sources above. Again, the ERF of the OPV-C cell studied is comparable to most other OPVs – it is neither among the best (having ERFs as high as 50) nor among the worst (having ERFs as low as, or lower than, 5).

7 Discussion

7.1 Reliability

The inventory data have been gathered from various sources. The ingoing materials have been gathered directly from the commissioner, whereas the R2R process energy has been quantified using proxies. For this reason, the energy use for the processes should not be seen as an exact account of the energy use, but as an indication of the fact that the processing has small overall impact compared to the input materials. In addition, some materials were exchanged by proxies, which further adds to the uncertainty. One such example is using data for graphite instead of graphene for the carbon electrodes.

Regarding the background system, there is some uncertainty regarding the results of the sputtering process. Although the data was gathered directly from manufacturer by Espinosa et al. (2012a), the uncertainty lies within whether this is a correct estimate for the barrier substrate investigated in this study. The estimate does, however, indicate that, as expected by the commissioner, the sputtering process makes up a substantial share of the overall energy use and the environmental impact.

In addition, the current intended application for the OPV-C is indoor applications. This means that the solar cells are not likely to gather their light from direct sunlight, but rather from indoor lighting. Thus, the results derived from assumptions for insolation (EPBT and ERF), should be seen as guiding values and a first simplified comparison between large-scale application of the studied OPV-C and other OPVs. To assess a specific application and the impact of replacing, for example, a battery with a small solar cell in indoor application, it can be more useful to base an assessment on a functional unit such as “area of solar cell replacing one battery” for some specific application.

7.2 Areas of Improvement

The results clearly show that the PET barrier substrate is the part of the solar cell with the largest contribution to all impact categories. Thus, a reasonable next step is to focus on this material. Other OPV technologies have significantly less CED due to the fact that they do not use a sputtered barrier substrate. This is a trade-off problem, as the protective barrier might increase the lifetime of the solar cell, which is imperative for customer satisfaction and the product’s viability on the market. However, a solar cell with significantly less CED would also have a significantly shorter EPBT. Regarding the ERF, it is not clear that the solar cell would benefit from a lower CED if it also has a negative impact on the longevity, but other studies of OPVs have shown that ERFs higher than those obtained in this study are possible to reach.

As noted in Section 6, the electricity mix used in both the foreground and background processes plays a significant role for the total emissions and environmental impacts. Electricity mixes with a sizable portion of fossil energy result in substantially more greenhouse gases and other emissions, which subsequently results in electricity-intensive processes that cause a large portion of the climate change and other environmental impacts. Thus, the electricity mix for the sputtering process has a significant impact on the emissions, and the manufacturing site and the electricity it uses can be further investigated. Since the use of electricity from fossil sources largely increases the final environmental footprint of the OPV-C, it is desirable to have a supplier that uses non-fossil electricity sources for the production, at least for the sputtering process.

Other ways of reducing the environmental impact is by increasing the efficiency in the manufacturing process. One area of improvement is the yield. By minimising the losses, both for ingoing inks but perhaps mainly in the conversion step, less scrapped material (and its environmental impact) is allocated to the final solar cell, reducing the overall environmental impact of the OPV-C. Another aspect to consider is increasing the active area of the solar cell, making a larger part of the PET barrier substrate useful for electricity production.

Regarding the photoactive layers, the active layers are the largest contributor to almost every impact category. One exception is terrestrial ecotoxicity, where the surfactant in the PEDOT-layer contributes substantially. With this exception, PCBM is the material with the largest environmental impact in the photoactive layers.

8 Conclusion

The largest single contributor to the CED is the PET barrier due to its energy intensive sputtering process. In total, the PET barrier substrate stands for 90% of the CED. A large portion of the input energy to OPV-C cell production is electric energy. For this reason, the total environmental impact of an OPV-C cell depends largely on the source of electricity used, partly in the foreground system, but mainly in the background processes. The higher the carbon footprint of the electricity used, the higher is the carbon footprint of the final product. If a German electricity mixed is assumed for the sputtering process, the total climate change impact of 1 m^2 active area solar cell is almost 54 kg CO_2 equivalents, whereas using a Swedish electricity mix for the sputtering process would lower the climate change impact with 90%, releasing less than 6 kg CO_2 equivalents per 1 m^2 active area OPV-C.

Another factor that has a strong impact on the final environmental footprint of the product is the production yield. Decreasing losses in the conversion step by utilizing as much of the processed area as possible can be a very effective way of minimising the carbon footprint, as no changes need to be done to the actual production or materials choice for the product.

A future scenario of large-scale electricity production was created for calculating the EPBT and the ERF of OPV-C. This showed that the EPBT is 16 months for a module with 5% efficiency, and less than 8 months for a module with 10% efficiency. Other studies of OPVs show EPBTs between 2.5 months and 4 years. The ERF, assuming 10-year lifetime of a module, is 7.6 for a module with 5% efficiency and 15.1 for a module with 10% efficiency. Other studies of OPVs showed ERFs between 7.5 and 51.

In conclusion, there are three main points of improvement for the OPV-C manufacturing. The primary area to consider for improvement of the CED and subsequently all impact categories, as well as the EPBT and the ERF, is the PET barrier substrate. The most influential change would be to find a substitution for the current substrate with a less energy intensive manufacturing process. If this is not possible, the second suggestion of improvement is to use a substrate barrier produced with low-fossil electricity, as this would lead to significantly lower environmental impacts for the OPV-C compared to one produced with fossil-intense electricity. Third, reducing the losses in the conversion step is another way to reduce the CED and the environmental impact of the OPV-C technology.

9 References

Acero, A. P., Rodríguez, C., & Changelog, A. C. (2015). *LCIA methods Impact assessment methods in Life Cycle Assessment and their impact categories*. Retrieved from http://www.openlca.org/files/openlca/Update_info_open

Anctil, A. (2011). *Fabrication and Life Cycle Assessment of Organic Photovoltaics*. Retrieved from https://scholarworks.rit.edu/cgi/viewcontent.cgi?referer=https://www.google.com/&httpsredir=1&article=5326&context=theses

Anctil, A., Babbitt, C. W., Raffaelle, R. P., & Landi, B. J. (n.d.). *Supporting Information for LIFE CYCLE IMPLICATIONS OF FULLERENE PRODUCTION*. Retrieved from https://pubs.acs.org/doi/suppl/10.1021/es103860a/suppl_file/es103860a_si_001.pdf

Anctil, A., Babbitt, C. W., Raffaelle, R. P., & Landi, B. J. (2011). Material and energy intensity of fullerene production. *Environmental Science and Technology*, *45*(6), 2353–2359. https://doi.org/10.1021/es103860a

Baumann, H., & Tillman, A.-M. (2004). *The hitch hiker's guide to LCA : an orientation in life cycle assessment methodology and application*. Retrieved from http://eds.b.ebscohost.com/eds/detail/detail?vid=1&sid=5e67d3dd-ace8-4e4a-bea9-10cd3a471262%40pdc-v-sessmgr02&bdata=JnNpdGU9ZWRzLWxpdmUmc2NvcGU9c2l0ZQ%3D%3D#AN=clc.b1274116&db=cat06296a

Bourzac, K. (2018). Organic solar cell smashes performance record. Retrieved March 21, 2019, from https://cen.acs.org/energy/solar-power/Organic-solar-cell-smashes-performance/96/web/2018/08

Buckley, P. (2009). Solarmer Energy claims world record efficiency for plastic solar cells | EE Times. Retrieved March 12, 2019, from https://www.eetimes.com/document.asp?doc_id=1256114

ecoinvent 3.5 – ecoinvent. (2018). Retrieved July 8, 2019, from https://www.ecoinvent.org/database/ecoinvent-35/ecoinvent-35.html

Energuide. (2019). What is the kilowatt-peak? – Energuide. Retrieved June 5, 2019, from https://www.energuide.be/en/questions-answers/what-is-the-kilowatt-peak/1409/

Espinosa, N., García-Valverde, R., & Krebs, F. C. (2011). Life-cycle analysis of product integrated polymer solar cells. *Energy and Environmental Science*, *4*(5), 1547–1557. https://doi.org/10.1039/c1ee01127h

Espinosa, N., García-Valverde, R., Urbina, A., & Krebs, F. C. (2011). A life cycle analysis of polymer solar cell modules prepared using roll-to-roll methods under ambient conditions. *Solar Energy Materials and Solar Cells*, *95*(5), 1293–1302. https://doi.org/10.1016/j.solmat.2010.08.020

Espinosa, N., García-Valverde, R., Urbina, A., Lenzmann, F., Manceau, M., Angmo, D., & Krebs, F. C. (2012). Life cycle assessment of ITO-free flexible polymer solar cells prepared by roll-to-roll coating and printing. *Solar Energy Materials and Solar Cells*, *97*, 3–13. https://doi.org/10.1016/j.solmat.2011.09.048

Espinosa, N., Hösel, M., Angmo, D., & Krebs, F. C. (2012). Solar cells with one-day energy

payback for the factories of the future. *Energy and Environmental Science*, *5*(1), 5117–5132. https://doi.org/10.1039/c1ee02728j

Espinosa, N., & Krebs, F. C. (2014). Life cycle analysis of organic tandem solar cells: When are they warranted? *Solar Energy Materials and Solar Cells*, *120*(PART B), 692–700. https://doi.org/10.1016/j.solmat.2013.09.013

Espinosa, N., Laurent, A., dos Reis Benatto, G. A., Hösel, M., & Krebs, F. C. (2015). *Supporting Information Which electrode materials to select for more environmentally-friendly organic photovoltaics?* Retrieved from http://minerals.usgs.gov/minerals/pubs/commodity/copper/mcs-2014-coppe.pdf

Espinosa, N., Lenzmann, F. O., Ryley, S., Angmo, D., Hösel, M., Søndergaard, R. R., … Krebs, F. C. (2013). OPV for mobile applications: An evaluation of roll-to-roll processed indium and silver free polymer solar cells through analysis of life cycle, cost and layer quality using inline optical and functional inspection tools. *Journal of Materials Chemistry A*, *1*(24), 7037–7049. https://doi.org/10.1039/c3ta01611k

Finnveden, G., Hauschild, M. Z., Ekvall, T., Guinée, J., Heijungs, R., Hellweg, S., … Suh, S. (2009). Recent developments in Life Cycle Assessment. *Journal of Environmental Management*, *91*(1), 1–21. https://doi.org/10.1016/j.jenvman.2009.06.018

García-Valverde, R., Cherni, J. A., & Urbina, A. (2010). Life cycle analysis of organic photovoltaic technologies. *Progress in Photovoltaics: Research and Applications*, *18*(7), 535–538. https://doi.org/10.1002/pip.967

Geiker, M. R., & Andersen, M. M. (2009). Nanotechnologies for sustainable construction. *Sustainability of Construction Materials*, 254–283. https://doi.org/10.1533/9781845695842.254

Gevorgyan, S. A., Bundgaard, E., García-Valverde, R., Helgesen, M., Hösel, M., Heckler, I. M., … Carlé, J. E. (2017). Overcoming the Scaling Lag for Polymer Solar Cells. *Joule*, *1*(2), 274–289. https://doi.org/10.1016/j.joule.2017.08.002

Goedkoop, M., Heijungs, R., Huijbregts, M., De Schryver, A., Struijs, J., & van Zelm, R. (2013). ReCiPe 2008. A life cycle impact assessment method which comprises harmonised category indicators at the midpoint and endpoint level. *Dutch Ministry of Housing, Spatial Planning and Environment (VROM): The Hague*.

Grandell, L., & Höök, M. (2015). Assessing Rare Metal Availability Challenges for Solar Energy Technologies, (September). https://doi.org/10.3390/su70911818

Groenendaal, B. L., Jonas, F., Freitag, D., Pielartzik, H., & Reynolds, J. R. (2000). Poly(3,4-ethylenedioxythiophene) and Its Derivatives: Past , Present , and Future. *Advanced Materials*, *12*(7), 481–494. https://doi.org/10.1002/(SICI)1521-4095(200004)12:7<481::AID-ADMA481>3.0.CO;2-C

Günes, S., & Sariciftci, N. S. (2017). *Organic and inorganic hybrid solar cells*. *Printable Solar Cells*. https://doi.org/10.1002/9781119283720.ch1

Hellweg, S., & Canals, L. M. I. (2014). Emerging approaches, challenges and opportunities in life cycle assessment. *Science*, *344*(6188), 1109–1113. https://doi.org/10.1126/science.1248361

Hengevoss, D., Baumgartner, C., Nisato, G., & Hugi, C. (2016). Life Cycle Assessment and eco-efficiency of prospective, flexible, tandem organic photovoltaic module. *Solar*

Energy, *137*, 317–327. https://doi.org/10.1016/j.solener.2016.08.025

Kim, H. C., & Fthenakis, V. (2013). Life cycle energy and climate change implications of nanotechnologies: A Critical Review. *Journal of Industrial Ecology*, *17*(4), 528–541. https://doi.org/10.1111/j.1530-9290.2012.00538.x

Klöpffer, W., Mary, ·, Curran, A., Hauschild, M. Z., & Huijbregts Editors, M. A. J. (2015). *LCA Compendium-The Complete World of Life Cycle Assessment Series Editors: Life Cycle Impact Assessment*. Retrieved from http://www.springer.com/series/11776

Krebs, F. C. (2009). Fabrication and processing of polymer solar cells: A review of printing and coating techniques. *Solar Energy Materials and Solar Cells*, *93*(4), 394–412. https://doi.org/10.1016/j.solmat.2008.10.004

Krebs, F. C., dos Reis Benatto, G. A., Laurent, A., Hösel, M., & Espinosa, N. (2015). Which Electrode Materials to Select for More Environmentally Friendly Organic Photovoltaics? *Advanced Engineering Materials*, *18*(4), 490–495. https://doi.org/10.1002/adem.201500509

Lee, T. D., & Ebong, A. U. (2017). A review of thin film solar cell technologies and challenges. *Renewable and Sustainable Energy Reviews*, *70*, 1286–1297. https://doi.org/10.1016/j.rser.2016.12.028

Lunardi, M. M., Ho-Baille, A. W. Y., Alvarez-Gaitan, J. P., Moore, S., & Corkish, R. (2017). A life cycle assessment of perovskite/silicon tandem solar cells. *Progress in Photovoltaics*, (October 2011), 156–172. https://doi.org/10.1002/pip

Marinova, N., Valero, S., & Delgado, J. L. (2017). Organic and perovskite solar cells: Working principles, materials and interfaces. *Journal of Colloid and Interface Science*, *488*, 373–389. https://doi.org/10.1016/j.jcis.2016.11.021

Meng, L., Zhang, Y., Wan, X., Li, C., Zhang, X., Wang, Y., … Chen, Y. (2018). Organic and solution-processed tandem solar cells with 17.3% efficiency. *Science (New York, N.Y.)*, *361*(6407), 1094–1098. https://doi.org/10.1126/science.aat2612

Newman, D. (2018). Organic solar cells reach record efficiency, benchmark for commercialization | University of Michigan News. Retrieved March 21, 2019, from https://news.umich.edu/organic-solar-cells-reach-record-efficiency-benchmark-for-commercialization/

Nothingserious. (2016). Structure of PCBM, omitting the hidden carbons. *Wikipedia*. Retrieved from https://commons.wikimedia.org/wiki/File:PCBM_simple.svg

Rafique, S., Abdullah, S. M., Sulaiman, K., & Iwamoto, M. (2018). Fundamentals of bulk heterojunction organic solar cells: An overview of stability/degradation issues and strategies for improvement. *Renewable and Sustainable Energy Reviews*, *84*(December 2017), 43–53. https://doi.org/10.1016/j.rser.2017.12.008

Raugei, M., Fthenakis, V., & Kim, H. C. (2011). *Methodology Guidelines on Life Cycle Assessment of Photovoltaic Electricity IEA-PVPS Task 12 View project Multiple Myeloma View project*. Retrieved from https://www.researchgate.net/publication/268212388

Roes, A. L., Alsema, A. L., Blok, K., & Patel, M. K. (2009). Ex-ante Environmental and Economic Evaluation of Polymer Photovoltaics, (January 2012), 2–6. https://doi.org/10.1002/pip

Schmidt-Mende, L., & Weickert, J. (2016). *Organic and Hybrid Solar Cells*. *Organic and Hybrid Solar Cells*. https://doi.org/10.1515/9783110283204

Søndergaard, R., Hösel, M., Angmo, D., Larsen-Olsen, T. T., & Krebs, F. C. (2012). Roll-to-roll fabrication of polymer solar cells. *Materials Today*, *15*(1–2), 36–49. https://doi.org/10.1016/S1369-7021(12)70019-6

Song, Y., Chang, S., Gradecak, S., & Kong, J. (2016). Visibly-Transparent Organic Solar Cells on Flexible Substrates with All-Graphene Electrodes. *Advanced Energy Materials*, *6*(20), 1600847. https://doi.org/10.1002/aenm.201600847

Than, K. (2018). Critical minerals scarcity could threaten renewable energy future. Retrieved March 11, 2019, from https://earth.stanford.edu/news/critical-minerals-scarcity-could-threaten-renewable-energy-future#gs.10204q

Tsang, M. P., Sonnemann, G. W., & Bassani, D. M. (2016). Life-cycle assessment of cradle-to-grave opportunities and environmental impacts of organic photovoltaic solar panels compared to conventional technologies. *Solar Energy Materials and Solar Cells*, *156*, 37–48. https://doi.org/10.1016/j.solmat.2016.04.024

Tsang, M., & Sonnemann, G. (2016). *Life-cycle Assessment of 3rd-Generation Organic Photovoltaic Systems: Developing a Framework for Studying the Benefits and Risks of Emerging Technologies*. Retrieved from https://tel.archives-ouvertes.fr/tel-01485786/document

Tsang, M., Sonnemann, G. W., & Bassani, D. M. (2015). A comparative human health, ecotoxicity, and product environmental assessment on the production of organic and silicon solar cells. *Prog. Photovolt: Res. Appl.*, *17*(November), 115–125. https://doi.org/10.1002/pip

Ungvarsky, J. (2019). Fullerene: Discovery Service for Chalmers University of Technology. Retrieved May 15, 2019, from http://eds.b.ebscohost.com/eds/detail/detail?vid=4&sid=9679e282-3b8b-49a3-b4b4-4ac85c480589%40sessionmgr120&bdata=JnNpdGU9ZWRzLWxpdmUmc2NvcGU9c2l0ZQ%3D%3D#AN=87321421&db=ers

Wernet, G., Bauer, C., Steubing, B., Reinhard, J., & Moreno-Ruiz, E. Weidema, B. (2016). The ecoinvent database version 3 (part I): overview and methodology. *The International Journal of Life Cycle Assessment*, *21*(9). https://doi.org/1218-1230